Reply on Review Process of acp-2017-472 Version 1

L. Schoon and Ch. Zülicke

October 4, 2017

First of all, we like to thank the two anonymous referees for their time expenses to comment on our manuscript acp-2017-472 published in the discussion part of the special issue of Atmospheric Chemistry and Physics "Sources, propagation, dissipation and impact of gravity waves" on 3 July 2017. In the following we first give an overview of the main changes of the manuscript, adressing both referees and the editor (Sec. 1). After that, we reply in detail on the constructive comments of Referee #1 (Sec. 2), followed by the respondence to the statements of anonymous Referee #2 (Sec. 3).

1 General Comments of the Authors

- Regarding the suggestion of Referee #2 to "improve the whole text" the authors decided to rewrite the whole manuscript. Therefore, the attached file including the highlighted changes looked very complex and we omitted it.
- Now, we attempt to guide the reader to the impact of our manuscript by highlighting more intensively its novel characters in the introductionary part. We expanded the literature research massively.
- As Referee #2 had concerns regarding the reliability of our data (preprocessed with the WRF Preprocessing System (WPS)) we thoroughly investigated the analysis data of the European Centre for Medium-Range Weather Forecasts (ECMWF) to find the best fitting data set and resolution of data during the last month. All calculations were redone and restricted to altitudes below 45 km to avoid the strong

sponge layer in ECMWF data starting at 1 hPa, following the suggestion not just of Referee #1 but also published findings in literature (Sec. 2.3). We avoid horizontal interpolation by keeping the data on the original latitude-longitude grid, adjusting our algorithm accordingly. The discussion on ECMWF data is shortended appreciably in favour of a brief literature review.

- We provide a step-by-step outline of the methods because Referee #2 doubts that the former explanation was sufficient (Sec. 2.1). We also add some calculations in the Appendix.
- Now, the application of the method is clearer arranged and trimmed to the analysis of three profiles from one time step (Sec.3).
- The concerns of Referee #2 regarding our pictoral schemes of hydromechanics, namely "valves and pumps" are taken care of. We erased this literal description of the analysed mechanisms from the manuscript.

We want to highlight again, that this manuscript focuses on the introduction of our novel method called "Unified Wave Diagnostics" (UWaDi). The application on the minor Sudden Stratospheric Warming on 30 January 2016 acts as a demonstrative application to show the advantage of this method. We plan to join the closer analysis of observations and models with respect to local features of GW generation and propagation. The authors highly recommend, that the introduction and the application of UWaDi should not be seperated and published in different journals as we prefer to join the special issue (SI) "Sources, propagation, dissipation and impact of gravity waves". All four issues named in the title of this SI are specifically addressed in the discussion part of our manuscript. Furthermore, we hope by belonging to this SI, that other scientists interested in this topic can find simple access to our method and cooperation.

2 Comments to the Referee #1

1. Filter and filter response
At page 7, line 10 you introduce that you use a bandpass filter. You state the filter limits in terms of wavelengths. However, most filters have a spectral response rather than a hard limit. For the further interpretation this response is important. In particular, the short horizontal wavelengths cut-off might remove part of the mountain waves and favor waves excited by spontaneous imbalance and the long vertical wavelength cut-off could

remove part of the GW spectrum in the high wind case (22 January). The latter would mean that you underestimate GWs for this case. Therefore please include a figure showing the filter response in terms of wavenumber or wavelength. In general, please explain why you need this filter at all.

The bandpass filter acts in spectral space, where we sort out waves that are not important for our analysis. Here, we use a rectangular filter with hard limits of k_{min} and k_{max}. UWaDi can be run with a gaussian shape bandpass filter, which does not have sharp limits. However, we find best results with the rectangular filter in this case.
We now choose a range of wavelengths between 100 km and 1500 km horizontally and 1 km and 15 km vertically. We find inertia GWs from spontaneous imbalance and flow over orography, as we discuss in Sec. 4 of the new manuscript. Insofar, the filter is wide enough. The bandpass filter is described a bit more in detail in Sec. 2.1, Step 4. We also performed numerous tests with the sensitivity of the results to the filter and resolution of data (grid sizes of 1°, 0.36° and 0.1°). It turned out, the characteristic wavelength mentioned in the manuscript does not depend on grid size and filter width. However, we did not dwell on these details in the manuscript, for the sake of brevity.

2. Discuss the advantages and disadvantages of the technique
All techniques to analyze waves need to make a trade off between spectral and spatial resolution. The Hilbert transform is an innovative and elegant concept for high spatial resolution. Since one of the major objects of the paper is to introduce the new technique you should have a paragraph highlighting the properties of the new method. If I understand this correctly, the advantages are:

- *The tool is mathematically well defined*
- *It is applicable to data of any dimension 1D to 4D*
- *Beside some spectral filter it does not make a preselection of the wavelengths, i.e. it is superior to e.g. Fourier transform, which works on a fixed grid and distributes spectral power from any other wavelengths to that grid, which needs to preset the analysis volume and thus either smears out waves with small wavelengths or becomes unreliable at large wavelengths*
- *With FFT behind, it is fast*
  The prize you have to pay:

- *You can determine only one wave vector per location, i.e. you attribute all the wave energy to a single wave. This does not allow to separate, for instance, the superposition of an upward and a downward propagating wave close to a reflection layer. (maybe that could be the reason for some peaks of wave action below the tropopause)*

- *With FFT behind some filter issues should apply*

According to this comment, we extended the method part in the introductary part as well as the method section itself (Sec. 2 to 2.2) where we discuss the above listed issues.

3. Introduce the idea
You could make better use of the introductory paragraph of section 2 and motivate the main idea of introducing the Hilbert transform. Perhaps something like: In this section we develop and validate an algorithm to extract wave parameters from equidistant three-dimensional data. For local diagnosis of waves, e.g. inertia gravity waves, phase-independent estimates of wave amplitudes as well as estimates of the wave vector are essential. For this we employ the Hilbert transform. The Hilbert transform shifts any sinusoidal wave structure by a quarter phase, i.e. turning a sine into a cosine. By constructing a new complex number consisting of the original field as real part and its Hilbert transform as the imaginary part, the absolute value is always the amplitude (square-root sum of sine and cosine), independent of the phase, the wavelength of the oscillation and without any explicit fitting of a wave. In addition the phase and, from the phase gradient, the wavenumber are determined. A tool called "Unified Wave Diagnosis" (UWaDi) is developed, which ..

Exceptionally minor changes, we have made use of this suggestion at the beginning of Sec. 2.

4. Graphics
Please use axis scaling which comprise all data. Quite frequently in your figures the curves run out of the selected value range. That is quite unnecessarily hampering the interpretation since often a small extension should suffice.

Because of the different data that we use now, we adapted the scaling of the axis and all corresponding figures are comparable.

5. Selection of individual profiles
The selection of individual profiles is somewhat arbitrary. With oblique wave propagation and finite vertical group velocity there may be other mechanisms contributing to the vertical structure than you would expect from a single column model. That should be noted in the text. In addition, profiles just in the vicinity seem to be quite different though similar filter arguments would apply. I think it would be more meaningful to select a longitude range of similar filter conditions and show the average profile for that range. Most of your conclusions would still hold and these are the valid ones. For the discussion of these profiles use the actual values (and not as sometimes now average values). For the critical wind filtering discussion you may assume upward propagation and then you should have a horizontal propagation direction and see whether a critical layer is approached.

We inserted the restriction of a vertical-only columnar propagation analysis in the introduction. Further, we checked if spatial averaging over a longitude range of similar wind filtering conditions affect our vertical profile approach. This was not the case so we want to keep our approach of local profiles to point out that we are able to find reliable wave quantities on every grid point without the necessity of spatial averaging. In detail, instead of the local profiles at 7.56° E, 151.92° E and 240.12° E we spatially averaged over 340-30° E, 125-180° E and 190-270° E and found no change in the overall results compared to our local analysis.

6. Remove inconclusive parts
You compare to radiosonde data and find that they are different. However, there are many reasons why this could be the case and a detailed discussion is beyond the scope of the paper. Similar, there is no reason why wave action should be Gaussian shaped in the altitude profile, so a comparison of peak altitudes is not physically plausible. Please remove these discussions.

We removed this parts from the manuscript. Furthermore, we added results from other publications which are more comparable to ours (e.g. Krisch et al. (2017)).

Specific comments:
P1L1 Why "maintain"? What do you want to say?

Except from a few spectral decomposition methods, the analysis of GWs is based on local methods, and at first reveals local wave phenomena. The calculation of zonal means then is a decision for generating a climatological mean state, but not a question

The abstract was rewritten. We distinguish our methods from other methods now clearer in the Introduction and the method part (Sec. 2-2.2): We want to have phase-independent local wave quantities.

P1L13 1000km (at the equator zonal wave 40) is more commonly called synoptic scale

We removed this.

P1L23 Complicated sentence

Changed

P1L24 "forbidden" is always a matter of the phase speed of the waves. Perhaps: as well as zones where wind reversals inhibit the propagation of GWs.

Changed

P1L25 "Models and simulations" That are not two equal terms to be linked by "and"; you need the model to perform a simulation.

It is removed.

P2L14 At altitudes below the sponge. Above about 40km GWs are very strongly damped and not realistic at all

We restrict our analysis to an altitude up to 45 km now. A discussion on the impact of the stratospheric sponge layer is given in Sec. 2.3 and Sec. 4.

P2L15 Even though the tropical portion of parameterised convective GWs is still too small Not clear what you want to say: ECMWF has a parametrization for convection. This likely results in a misrepresentation of the resolved subtropical/tropical gravity *waves. ECMWF does not use a specific parametrization for convective waves, only a non-orographic GW parametrization.*

This missunderstanding was removed.

P2L34 Other methods are 3D S-transform (Wright et al., ACP, in press), localized sinusoidal fits (Lehmann et al., AMT, 2012, Preusse et al., ACP, 2014) and 3D wavelets. These are more closely related to your own method and should hence be quoted here. These would be the methods you could delineate your own tool against in a separate paragraph.

We followed this suggestion in Sec. 2.2 and included a careful comparison for a test case. It revealed clearly the differences between the methods. We are very grateful to the Reviewer #1 for this particular suggestion.

P4L1 discrete Fourier transform

Changed

P4L4 ... a user-defined ... since you pronounce like "you" and not like "us", i.e. the word as pronounced starts with a consonant

Changed

P4L21 As I understand it, d is not the vector of spatial coordinates x,y,z as in the lines before (e.g. a[x,y,z]). Instead it corresponds to the spatial index of e.g. a wavenumber k_x for the x direction, i.e. the sums above are the sums over the three spatial dimensions. Correct? Please use different notations for different things.

Yes, you are correct. It is changed.

P4L24 The noise threshold is essential for understanding the results. How is that calculated? Globally? Locally? Please include the definition.

Now, the definition of the quality checks can be found in Sec. 2.1, Step 9.

P4L25 Why is this necessary after you have applied a band-pass filter already above?

The necessity of the low-pass filtering is now explained in more detail in Sec. 2.1, Step 8. Furthermore we provide a short explanation in Appendix A on that topic.

P5L4 A one- ...

The typo has been changed.

What happens for two waves of similar size in the same volume?

We now discuss the impact of a two-wave mixture in Appendix A.

P5L14 sufficiently monochromatic

This exact formulatin was rewritten in the new manuscript. We refer on the method sensitivity on spectral properties of the data mainly in the discussion part of the new manuscript. It is an important aspect, so we come back to it in several parts of the manuscript. In the step-by-step outline we mention that all variance is considered independent on the spectral properties. Problems may arise with the calculation of the wave number for wide spectra because for that the amplitude-weighted mean is taken. Special care is taken of this issue in the two-wave mixture calculation in the Appendix. In the Conclusion we give references regarding this issue.

P7 Please state precisely which data you are using. Though both Cy41r1 and Cy41r2 use T1279 the effective resolution is different and for Jan 2016 both versions were generated.

A precise description can be found in Sec. 2.3 now.

P7L4 restricted -> reduced

Not relevant any more.

P7L6 222km / cos(lat) for zonal direction; makes a factor of 2 at 60N and introduces *an anisotropy in the cutting frequency*

After a couple of tests with grids of 1°, 0.36° and 0.1°, now, we use data with a resolution of about 40 km horizontal grid distance (0.36°). With our lower bandpass limit of 100 km we make sure that we find waves that are resolved in the data. In order to acknowledge the latitude-dependence of the longitudinaldistance, we first take the meridional sectoin for which, from the lat-lon grid, we calculate the distance in this direction and apply the filter, FFT, etc. Because we operate separately with the three dimensions and respective filtering, we take this anisotropy into account.

P7L10 These limits are coarse. ECMWF resolves in both relevant model cycles mountain waves with wavelengths shorter than 200km, i.e. you have performed here a preselection in physics.

The lower limit is reduced to 100 km horizontally.

P7L23 ... but not interacting with the mean flow Is that true? A wave refracted horizontally would conserve its wave action, but change direction and thus transfer momentum to the mean flow.

We rewrote this part. The wave action is a conserved quantity describing waves in an inhomogeneous background wind field. It does not change for upward propagating waves, as long as they do not interact with the mean flow.

P7L26 in a mid- and low-frequency approximation:

Inserted

Say -> From

Changed.

P7L30 Please use always intrinsic and ground-based, respectively.

With first appearance of intrinsic and apparent we added the terms (flow-relative) and (ground-based) to clear this up.

P8L1 omit: "one has to accept that"

Yes. Done.

P8L3 for the following analysis primarily wave action is used.

Changed

P8L7 The period 21 January to 21 February 2016 exhibits interesting wind features and is chosen for further analysis.

Not relevant any more.

P8L8 zonal mean?

Not relevant any more.

A change in wave action is supposed to be caused by a variation in the intrinsic frequency hinting at a steepening of GWs You mean relative to energy? Steepening = longer vertical wavelengths

The steepening of waves regarding the vertical wave lengths is explained more in detail, now, in Sec.4.

Your analysis in F3 is 2D (in the horizontal plane)? Please highlight this.

Former Fig.3 has been removed.

P9L1 but not well above the filter!

Yes, this does not happen in this new analysis with different data. The largest wavelength, found in the mountain-wave case 1 is well inside the vertical filter of 1 km to 15 km.

P9LL1 What is the use of average values. In particular of e.g. average intrinsic phase speeds.

This discussion was removed.

P9L9 Here you do a cross-comparison with four differences: location, time, generic data and analysis method. This is very difficult to interpret. Better keep at least time and space the same.

Mentioned above, this discussion was replaced by a comparison to observations made during a comparable synoptic situation.

Figure 4: Please show also plots for wave action from UWADI

This can be seen in Fig. 2, now.

P9L24 Where is there any evidence for orographic waves in the figure?

This was removed.

In the stratosphere you can use the rule of thumb: 3km vertical wavelength correspond to 10m/s intrinsic phase speed. With a vertical cut-off of 15km that would mean that at 50m/s background wind speed most slow waves (such as mountain waves) are still in, and at 75m/s background wind speed a considerable part is removed.
Yes, we also did similar thumbs for any of our profiles to be sure we do not cut the GWs. Actually, the wind was not as large in the considered cases so we do not run into trouble.

How is a vertical wavenumber zero compatible with a long-wavelength filter edge of 15km?

Sorry, this was a bit loose writing. The algorithm does not return a Zero wave number. Now, we find the smallest wavelength (highest vertical wave number) in the stratospheric jet case 2 with 2 km. This is well in the limites of our filter (1 km to 15 km).

Show the filter response for the respective axes.

We experimented with overplotting the filter response over these already rather detailed plots. Unfortunately, we did not arrive at a satisfactory solution without causing confusion. So, we rather left it out.

Fig 6 Please use the same vertical axis for panels a and b

We do provide different profiles with similar axis in the new manuscript.

P11L13 "This finding contributes to our understanding to the density decrease with height which is not considered for the kinematic wave energy." Perhaps instead: The vertical profile results mainly from two competing effects: at increasing altitude density decreases. As the kinematic wave energy does not include density, we expect exponential energy growth for conservative wave propagation and hence a strong increase in regions of weak dissipation. Above 40km the mesospheric sponge of the ECMWF model sets in and cause strong, arteficial dissipation, which results in the decrease of wave energy at larger altitudes. In addition, ...

This was rewritten.

P11L15 Wave action should decrease above source altitude and there is no reason to assume it to be Gaussian. Please remove the sentence

With this little calculation we wanted to show that the energy maximum is always above the corresponding action maximum. Therefore, the Gaussian shape was taken as an arbitrary example for a function with maximum. However, as this calculation achieved more questions than clarity, we removed it.

P13L5 afterwards -> above

Not relevant any more.

P13L6 the slow westward

This was rewritten.

P13L9 This is mid frequency approximation. If you use further approximations, note in the text

This was added.

P13LL7 You use a single profile at one fixed time for your argumentation, but wave propagation may be oblique, requires time and the tropopause may cause partial reflection (what happens in the latter case?). Are your conclusions valid the same way for the profile at 40W? It would make much more sense to me to integerate over a small region.

We discussed the issue of local profiles vs. spatial averaging already above. Because we want to show the advantages of local estimates, we do not average over regions. For a rough interpretation of profiles, the columnar (vertical-only) thinking was helpful. We are aware of the more complicated horizontal and vertical propagation issues and mention this in the text.

P13L21 GWs are forbidden -> GW propagation is strongly inhibited. Unless $N^2 < 0$ you always have some GWs which may exist

This was rewritten.

P13L28 A longitudinal profile at 20° An altitude profile at 20° west ... Where do I see the wavelike structure in the figure?

This Figure was removed.

P13L32 wave guide A wave guide means keeping the wave between two reflection layers as you would have it e.g. at the tropopause or mesopause for short horizontal wavelength waves. Open-walve region?

We decided to remove the terms of hydromechanics in favour of a more distinguished style of writing.

P17L4 Split this up: The tool is applicable to ... Here we apply the tool on divergence *fields and limit towards long wavelengths thus isolating GWs. The procedure leads to re<liable results for synthetic test cases. As a first application we run it on operational analysis data of ECMWF for a stratospheric warming case.*

This was rewritten.

In future, the lack ... For comparing the phases you do not even need to have the Hilbert transform 4D. The most serious limitation is that you need ECMWF data at sufficient dense sampling which you could get from forecast data. For a first step you could assume upward propagation of the wave energy.

Yes, you are right. In some cases one may fix the direction of wave numbers with a-priori assumptions. E.g. this is done in Wright et al. (2017). For the vertical wave number upward propagation can be fixed. However, any method working on spatially can solve this sign problem in general. We note this in the new manuscript.

17LL14 You use a pump=source and valve picture. 1.) You should have an introducing sentence that this is a picture for a more complicated process. 2.) That's based on Ron Smith's ideas? Is there any peer-reviewed article to quote? 3.) While the valve summarizes the properties of a wind profile, source is already such a general expression. Is it necessary to introduce a new word? In particular since source could work already in such a hydraulic picture.

This terms are removed. See above (Sec. 1).

3 Comments to the Referee #2

(1) As a first impression, the paper reads as an attempt to combine the presentation of an analysis tool (called "UWaDi") for estimating kinematic gravity wave properties with the discussion of the gravity wave propagation during a prolonged period of minor SSWs. Unfortunately, I've to admit: This attempt totally fails as neither the analysis tool part nor the gravity wave analysis are substantial enough to allow for a combined scientific publication.

We are sorry for this impression. We revised the whole manuscript to better point out the base of our method as well as the result of our application on the minor SSWs on 30 January 2016.

(2) The methodology to retrieve gravity wave parameters is not convincingly introduced and clearly outlined for global 3D gridded data. Compared to solid and mathematically exact descriptions, e.g. provided by Zimin et al. (2003), the mathematical part is poor, see comments below. Especially, it is not necessary to repeat that the method is working for synthetic data as this was documented by others already.

It would be much more interesting to see the application of the method to gravity wave packets using 3D IFS analysis fields of horizontal divergence step-by-step. Essential parts are missing in the description: extraction of wave packets (not all regions of non-zero divergence belong to gravity waves) and proof that the extracted wave packets really satisfy the dispersion relationship.

Another point: The horizontal divergence is a quantity which can hardly be observed in the atmosphere. I miss a clear link to observable quantities like temperature fluctuations. There are published attempts, e.g. by Khaykin et al. (2015) 1 to do so. Without such a link, the whole analysis tool is probably handy for gridded data but gives no quantitative relation to observations in the real atmosphere.

We thank the reviewer to raise this issue. In response, we added a step-by-step outline of the method. The improvements compared to Zimin et al. (2003) are highlighted in the Introduction as well as in the method part (Sec.2-2.2). We see the necessity of showing that the method works for synthetic data because with that we can point out clearly, that not just the envelope of this wave packet is estimated correctly (like Zimin et al. (2003) showed) but also the wave number calculation at every grid point (which is novel work in UWaDi) works well. This only could be done by an example where the wave number is known in advance. Furthermore, this synthetic wave packet works well as test case for the comparison of several methods (Sec. 2.2).

As described above, we prefer the synthetic test case from Zimin et al. (2003) because with that we can truely show the gain of UWaDi. The discussion of wave quantities in Sec. 3 and 4 should make sure, that we deal with GWs that fulfill the dispersion relation.

With these specifications, we used the advantage of availability of the divergence in the analysis data, which directly made accessible the wavy ageostrophic motion without the need of filtering out the geostrophic modes.

As we point out, this method is developped for gridded data and not primarily for observations. Nevertheless, we added in Sec. 2.1, Step 1 that the method works for every variable on gridded data, if numerical or dynamical filters are approved to provide the fluctuations of the background flow. We choose the horizontal divergence to overcome the use of a numerical filter. Several studies, including the named Khaykin et al. (2015) (Plougonven et al., 2003; Zülicke and Peters, 2006; Limpasuvan et al., 2011; Dörnbrack et al., 2012, 2017) use the horizontal divergence as a dynamical indicator for GWs and so do we.

(3) The analysis of the minor SSW is totally incomprehensive. It is not clear what the relation between time/space is and which mean values, which locations are considered. There are several hypotheses formulated and statements given in the text which are not proven by results presented in the paper. Is there any progress in knowledge, new understanding compared to the results on selective wave transmission during SSWs published by Dunkerton and Butchart (1984) 2 ?

We are again sorry for this impression. We changed the whole analysis and hope that Referee #2 sees the connection of our results to the discussion, now. The differences to Dunkerton and Butchart (1984) are pointed out in the Introduction and discussion part of the paper. Shortly: Dunkerton and Butchart (1984) investigated parameterised GWs of a different range of wave length than we do. We concentrate on resolved GWs in analysis data and its vertical propagation through the middle atmosphere. This was not done in Dunkerton and Butchart (1984). In particular, we provide such a local analysis on every longitude which is not possible with such an accuracy with other methods. This has been demonstrated in Sec. 2.2 with the Zimin test case.

(4) The writing is often very sloppy and not precise. Definitions are modified without discussing the implications, see remarks about wave action. The whole style of the paper is essentially not acceptable for a scientific publication. There is a frequent mix between presenting of results and discussions which blurs the paper and makes reading more than difficult. Below, I give several examples without attempting to edit through the whole

text. This would take too much time and effort I cannot spend. I actually stopped reading and commenting after Sec. 3.2. This does not mean, afterwards is all fine. It just means, I see the action by the authors to improve the whole text.

Generally, I noticed a tendency to name, denote facts and processes with new, partly fancy terms (mostly taken from hydromechanics for what reason ever) which are not exactly defined or explained in the text and which leave room for associations. I just want to remind the authors on one principle, scientific publications should follow. It is known as Occam's razor and says "Entities must not be multiplied beyond necessity". It would be great, if the author could follow this principle in future publications. Take as an example the naming of the analysis tool. Why a new name is created for a well-documented methodology which has been obviously used several times before? Well, maybe for other scales and maybe also because an approximated form of wave action is calculated here, but it is absolutely not clear why this minor modification should be named with "Unified Wave Analysis". What does "unified" mean?

The quality and labeling of some of the figures is poor. Examples are given below.

We take care of this remark and rewrote the whole text. Results (Sec. 3) and Discussion (Sec. 4) are clearly seperated, now. We hope that by reading the whole manuscript, the Referee will see our effort of answering the questions asked in the Introduction, analysed and discussed in Sec. 3 and 4 and summed up in Sec. 5. We carefully took care to keep the golden threat.

We removed the terms "valve and pump" because they seem to take away the attention from our scientific goals which is to point out the longitude-dependent vertical propagation of GWs. The name of the tool is not disputable. The unified character comes from several issues. First, the method is applicable to several different parts of wave types, e.g. GWs or Rossby Waves. Furthermore, any kind of variable can be analysed, as long as it contains wave-like structures. By choosing narrow band bandpass limits one can even analyse different kinds of one wave type. Hence, it can be used for any kind of gridded data. It is applicable on one-dimensional data and up to four dimensional data. We obtain phase-independent wave quantities which makes it easy to calculate wave energy measures locally. Again, our method is based on that one introduced by Zimin et al. (2003) but comes with an extra wave number estimation in all three dimensions

(which is the major novelty) and combines the three dimensional amplitude and wave number estimates on the same grid as the input data.
The Figures are new. The labeling is taken care of.

5) Essential references are missing in the text. The authors focus on the winter 2015/16. They totally ignore papers which are even published from authors of their own institution! Examples are given below.

Last but not least, clear-cut formulated scientific questions are missing for both parts of the paper. So, the suitability of the paper to fit within the scope of ACP cannot be evaluated so far. And maybe, to formulate scientific questions might be a suitable starting point for a new attempt to publish results of the presented study. Thus, at the end, I recommend to proceeds on two routes. First, outline the new facets of the wave analysis clearly and publish these as an independent methodological contribution, e.g. to the GMD. Secondly, conduct a thorough study of the sequence of minor SSWs which occurred in January/February 2016. If the increment of knowledge gain is measurable and constitutes a significant contribution to the understanding, such a paper would fit perfectly to ACP!

We extended the list of references to several publications regarding the Winter 2015/16.

As mentioned above, we reformulated the introduction to find scientific questions and tuned the whole text to answer those. Our comment on the seperation of the method and the application into two journals can be found above (Sec. 1).

Specific Remarks:
Abstract
line 1: These two sentences are incomprehensible. What do they mean? Furthermore, Abstract is not a place to argue.
line 2: Reads like a technical task which is the topic of the paper. Formulation and grammar is unclear: What is a "diagnostic tool for studies of wave packets locally"? Do you mean: "retrieve localized wave packets from 3D gridded data"? The following sentence with "UWaDi" confirms the impression of a technical study.
We hope the new formulation is clearer.
line 4: Be more specific: you use 6 hourly operational analyses of the IFS? Why do you

use such a general formulation as " ...is used to perform the analysis"? Write exactly what you do with the data: they are interpolated on a spatially equidistant grid to apply the Hilbert transformation to extract amplitudes and wave numbers at specific times ....
line 5: The first result appears (about the effect of the sponge layer). Is this an essential result of the applied method to be mentioned first? Does it undoubtedly relate to the assumed numerical damping or is there a possibility that the atmospheric state simply didn't supported gravity waves? See remarks to Sec.2.3.
line 7: Second result, however, incomprehensible again. What means "zonal mean wind quantities cannot reveal local 'valves' ...". The usage of not generally accepted terminology or terminology which is not yet introduced in the previous text is dangerous and does not explain anything. What are "zonal mean wind quantities"?
Line 8: third result: obviously, one event of the mentioned three cases (line 6) is picked randomly which states high gravity wave activity without any relation to location and height. And again a term "local pump" is used which does not explain anything. Why these relations to hydro-machines?
line 9: Why "Accordingly"? What shall the reader re-connect in order to conclude about the advantages which are stated?
At the end: The Abstract is incomprehensive and incomprehensible, and it leaves more questions than answers! It needs a thorough re-write and focus either on methodology or SSW dynamics.

Regarding the last suggestion of the Referee, we rewrote the abstract completely. There, all these comments were taken care of.

1 Introduction
Generally, an Introduction should contain the state-of-the-art knowledge of the topic which is going to be addressed in the paper. It should formulate the challenges and the methods which are applied to answer the scientific questions resulting from the challenges. At the end, the answers are given in the Conclusions where you should clearly state what kind of new knowledge has been generated by the research conducted for the paper. Unfortunately, this Section 1 only partly serves this purpose.

We extended the Introduction, including more information on other methods and analyses of the winter 2015/16. We resorted it and took care of rising questions in the individual paragraphs and answering them in the corresponding paragraph of the Conclusion.

First paragraph
PAGE 1
line 12: provide evidence by adding essential references

The authors clearly point out, that an overall overview on the different scales of GWs can be found in the given reference (Fritts and Alexander, 2003).

line 12/13: The logic of the sentence goes wrong: Do "the scales of GWs ... create a broad field of interest .."?? I don't think so. Furthermore, do you really claim that atmospheric gravity waves exist at 10 m scale??

No, we do not claim that. We reformulated the sentence to make its point clearer.

line 14/15: What do you mean with "huge changes in GW appearance"? Where? When? Increase? Decrease? Provide evidence by references. Be more specific. For example, mention that you consider the Northern hemisphere only and specify the physical variables you are referring to.

The new Introduction is clearer.

line 15/16: This classification relies on the definition of "normal winter conditions" and "summer-like conditions". Specify what is meant! Which months are you referring to? Early winter, late winter? The use of these terms is an example where the application of the principle of Occam's razor would be beneficial.

We are more specific now.

Essential references about SSWs are missing, also at lines 18-20. Start with
Butler, A.H., D.J. Seidel, S.C. Hardiman, N. Butchart, T. Birner, and A. Match, 2015: Defining Sudden Stratospheric Warmings. Bull. Amer. Meteor. Soc., 96, 1913–1928, https://doi.org/10.1175/BAMS-D-13-00173.1
and find relevant references therein.

We included more references on SSWs, especially those dealing with GWs. See paragraph 6 of the Introduction.

line 17: What are "winder" conditions?

This typo is removed.

lines 21-23: Very colloquial language! Be specific what the "crucial role in driving ..." means

Rewritten.

lines 23-25: Be more specific, not so general. Attention by using the term "wave guide": in the cited paper (Dunkerton and Butchart, 1984) this term never appears and, mostly, it refers to horizontal propagation. I think you might refer to the concept of selective wave transmission instead which was introduced by Dunkerton and Butchart (1984). Again: very colloquial language.

Rewritten

line 25: This is a rather general statement. Ask yourself what specific facts, information do we need from the cited papers for introducing your research topic! Just the statement that their data can be analyzed seems to weak!

We extended this.

PAGE 2
line 2: Do De Wit et al and the other cited papers really "verify" the momentum fluxes analyzed by the mentioned modeling papers? Be more specific and keep an eye what is needed in your text. As far as I see, momentum flux does not play any role in the paper!

We removed the references regarding the momentum flux.

line 4:
- The statements of the Ern et al. (2016) seem to be essential: Describe what is exactly

meant with the "zonal average view of GW parameters". Then, get the way to your point of local wave quantities.
- provide evidence of your statements using "mainly extracted" and "misleading"
Now, we point out clearly the advantage of our local method in the Introduction.

line 5: the fact that "local GW activity can vary locally" is known and best expressed in the intermittency which was derived from various observations - why such a long chain of arguments before??

This is rewritten.

line 6: colloquial: "gravity waves slow down" – be more physically exact and refer to vanishing vertical group velocity. Not all gravity waves interact with the critical level, only those whose phase speed is equal to the background wind. Good references are text books on gravity waves as Nappo (2012), Sutherland (2010), Gill (1982), Gossard and Hooke (1975), ... or the papers of Bretherton (1966, 1969) 3 and Booker and Bretherton (1967) 4 .

A discussion on critical layer absorption can be found in Sec. 4.

line 7 and 8: Introduce and explain physically what is meant by the used terms ("valve" and "bottleneck" and "pump") as you are now making the step from background conditions to local flow regimes.

For above mentioned reasons we removed these terms.

line 8 and 9: statement of the goal of this study, I suppose. Why test case? What is the emphasis of this study? Is it the methodology or the analysis of the minor SSWs? Focus on one or the other. To keep both alive does not work!

We clearly state our goals in the Introduction, now. More comments on that can be found in Sec. 1 above.

Altogether, the whole first paragraph contains too many aspects which do not logically lead to a clear goal formulated in terms of scientific questions. Even the last sentence *leaves it open what the paper is focusing on. It does not become evident what the scientific problem is nor why it is timely to conduct such an analysis being presented in the paper. There are vague associations that some kind of previous wave analysis is giving results which will be contrasted (improved, complemented??) with the results of this study. But, at the end, the paragraph is not saying this explicitly and remains incomprehensive.*

We are sure that the Introduction is clearer to the reader, now.

Second paragraph
line 10/11: a very general statement that combines too many aspects: Specifiy the data you are going to analyse! What is meant by "local phenomena and their coupling"? Give evidence for the statement ".. resolve essential parts of GW dynamics .." - in which sense essential?

A detailed description on the data can be found in Sec. 2.3.

line 11/12: provide reference, why already? What is meant with "correct GW appearance"??

The reliability of the data is discussed in the Introduction, as well as in the Sec. 2.3.

line 13/14: why the link to the tropics is necessary? Refer specifically to the results of Yamashita et al. if they are relevant for the present study.

We refer to Yamashita et al. (2010) and removed the link to the tropics.

lines 14-20: provide evidence for the ".... bigger portion of resolved GWs ....", this is just a statement, are there references? The collected arguments and statements do not convincingly lead to the concluding sentence starting with "Hence, ...". First of all, the requirements were never specified before. Secondly, the term "local valves" is not defined yet.

This is rewritten.

I'm trying to guess: you claim that the IFS data provide the locations of wave-induced

critical levels?? This might be true if one would know of which part of the GW spectrum you are talking about. Essentially, this aspect of resolution dependence should be discussed in detail to provide fair ground for further arguments. The presented arguments are too general. Moreover, there are quite a few case studies of the recent years using high-resolution analyses and forecasts of the IFS to derive local wave parameters, just to name a few:
Zhao, J., et al., 2017: Lidar observations of stratospheric gravity waves from 2011 to 2015 at McMurdo (77.84 S, 166.69 E), Antarctica: Part I. Vertical wavelengths, periods, and frequency and vertical wavenumber spectra. J. Geophys. Res., DOI: 10.1002/2016JD026368
Ehard, B.,et al, 2017: Horizontal propagation of large-amplitude mountain waves in the vicinity of the polar night jet, J. Geophys. Res., Atmos., 122, doi:10.1002/2016JD025621

We are aware of these publications and decided to add also several other studies that highlight local GW features. Especially in the last but one paragraph of the Introduction we deal with the ECMWF data. Furthermore, we made several case studies with respect to resolution and filters to find the best fitting data to our analysis (See Sec. 2.3). There the restrictions of the data are discussed, too. In particular, we found the same results using the 100 km to 1500 km filter for 0.36° and 0.1° grid size data. We interprete this finding with a GW spectrum which is rapidly decaying for horizontal wavelengths above 200 km.
Zhao et al. (2017) used ECMWF model data as background wind information to interprete vertical wavelengths from their lidar observations at McMurdo, Antarctica. For their spectral GW analysis the height range of 30 - 50 km was used. With regard to method, we quote some more complicated approaches, while for the application we focus on the SSW. Hence, for the sake of brevity we do not include this paper.
Ehard et al. (2017) concentrate on the GW behaviour above NZ and traced horizontally refracted GW signals in IFS data. However, in order to better focus the introduction to the considered SSW case, we quote this paper without further details in the introduction as an example for horizontal propagation.

lines 19-21: It is not convincingly explained why such an analysis is necessary. And what does such an analysis add to the understanding of internal gravity waves? What are the challenges? Why is such an analysis necessary?

We point out the impact of our analysis at the end of the most paragraphs in the introduction, now.

Again: also the second paragraph should be much better structured and focused on the needs which lead to the presentation of the presented approach to analyze gravity waves

We did that.

Third paragraph:
lines 22-line 9(PAGE 3):
This paragraph starts with sentences about sources (why not name them as non-orographic sources) and at line 24 it jumps to methods to extract wave properties: I would recommend to separate these both issues.
- what means "varying" in "search for varying GW sources": different, variable, transient, ...? Regarding the logics in the first sentence: Why is there "Another issue ... because there is some likeliness of ..."? No idea what this means and implies
- I don't like the formulation " ... which may 'pump' them into the middle atmosphere .." Why "pumping"? Why this analogy to hydro-machines? Waves are excited and they propagate in response to the ambient properties (wind, stability) of the medium. Physically, there exists an established terminology: vertical flux of wave energy or wave action (see again: Occam's razor).

This was rewritten, taken care of this comments.

line 25: provide evidence by proper references (" .. found in the literature."); the 2nd sentence in this line, and the following one too, remain incomprehensible as nobody knows what are you referring to. Also, the concluding sentence starting with "Hence, .." (line 26) cannot be verified based on the information you provided.

Again, by rewriting we hope to clear up this part.

line 27 - 35: Explain why the mentioned methods are relevant for the present study. From reading this part and scanning through the mentioned papers, I've got the impression that essentially all methodology to derive " .. wave amplitudes and wave numbers .." is available. What is the challenge and the need to present another method? I might be misled, but: you as the authors are responsible to make clear what the community is *missing in terms of knowledge and/or methodology. And: what are you going to add with your paper to close this identified gap! This is not obvious from the present text.*

The novelty of our method was already mentioned above and is pointed out much clearer in the manuscript now.

PAGE 3
lines 1 -9: Again, it would be beneficial if the reader would be provided with more accurate information. For me, it is rather nebulous what is taken from the published methodology and what is missing and will be added here.

These issues are now included in the Introduction and Methodology section.

lines 10-18:
The two goals are reformulated: (1) a new method is introduced here "to obtain phase-independent wave properties locally"? What specifically is meant? Amplitudes only? and (2) "local valves" are going to be detected by considering the vertical GW propagation through the varying background conditions during a mSSW (abbreviation not introduced yet).
"valve detection" – explain exactly what you mean.
- Here, you state you use "reanalyses" (line 12) but later I learnt, these are the operational analyses. Consistency in naming required! This also refers to the new terms "prewarming, midwarming, and postwarming" phases (line 17). Are these the same periods as the stages mentioned earlier on page 1, lines 16,17)???

Most of the issues stated are removed from the text. The data is explained in detail. Abbreviations are introduced correctly.

2 Method and Data
Line 19-23: In a potential methodological paper, the very short technical description could be expanded by a code description. Otherwise, the hints to "autonomous" processing and plotting and user-defined namelist as elements of the actual code do not make sense here.

We extended the section by a step-by-step explanation of the method.

Section 2.1:
about the name "UWaDi", see above

Discussed above.

line 26: give the range of x-values

Done

lines 25/27: the Hilbert transform does not "provide a new complex series" – the complex values are determined by Eq. (1) by means of the Hilbert transformation

Changed.

the mathematical description is poor as the definitions of DFT and F are not given; are these the same formulae as in Zimin etal (2003)? As a matter of fact, the interested reader should be able to code your algorithm solely based on the equations you provide and on references which exactly point to ingredients you used – this is not possible with the provided information.

As mentioned above, we provide a step-by-step outline, now. As mentioned in the manuscript, the authors may provide the code to interested readers if this is wanted. Again, the agreement to Zimin et al. (2003) is solely restricted to the mathematical background, namely the Hilbert transform.

are the quantities calculated by Eq. (1) and (4) the same?

Yes, they are. However, Eq. (1) shows the idea of the Hilbert transform. Eq. (4) belongs to the stepwise implementation of the Hilbert transform.

PAGE 4, line 9: I don't think "maintain" is the appropriate verb here, the amplitude or magnitude of a complex number is simply defined as written in Eq. (5); I think, the formulation " .. gives an estimate of the local envelope ..." is not correct. Shouldn't it be the amplitude of the wave packet?

This is rewritten for better understanding.

line 23: “First” instead of “Fist”

Changed

Generally, the reference to wave packets and the identification of them is missing!!

We provide the synthetic test case as a simple application of the method. There we indentify wave packets. (Sec.2 to 2.2)

What is the physical meaning of the phase (Eq. 6) with respect to the wave groups?

The real and (Hilbert-derived) imaginary part of the function are used to change to an amplitude-phase representation. While the amplitude takes the maximum elongation of oscillations, the phase describes the changes in between. How often the phase is changing, this is proportional to the frequency (in time) or wave number (in space). Respective differentiation brings it up. When the wave group consists of many freuquencies, our estimate returns the amplitude-weighted mean of all (see appendix A).

In Eqs (8) and (9) indices “d” are used. Later, “d” is used as abbreviation for the vector of Cartesian coordinates.

This is changed.

The filtering and smoothing, and the quality checks are not explained in a transparent way!

We provide this in the step-by-step manual, now.

A concluding paragraph about the advantages of the new method would facilitate the understanding and judgment of the presented algorithm.

First advantages are mentioned in the Introduction, now. Further we added a Section where we validate our methods with other methods. This clearly showed the locally precise estimation of amplitude and wave number.

Section 2.2:
To conduct the presented tests was certainly necessary to code the algorithm properly. However, as the results are neither surprising nor new, I would recommend skipping this part. Instead, the application of algorithm to a 1D series of horizontal divergence along a constant latitude circle at some selected altitude (taken from the IFS data) would be a convincing test if the algorithm really retrieves wave packets and leads to a realistic estimate of amplitude and wavenumber.

We discussed this above. Only a synthetic test case with a-priori known "truth" can be used to validate a method for itself and to conduct a qualified comparison to other methods.

Section 2.3:
PAGE 6
line 18: "ca." ???

Removed

PAGE 7
It appears that the authors only have limited information and knowledge about the physical parametrizations and the additional filtering and damping in numerical weather prediction models, especially, the IFS cycle they have chosen for their analysis. The main part of the damping in the stratosphere is due to the non-orographic wave drag formulation introduced several years ago (Orr et al., 2010) 5 . Terms as "stratospheric sponge" and "mesospheric sponge" do not describe properly what is done in the model integrations. Essential references are missing which describe the older status of filtering and damping (Jablonowski and Williamson, 2010) 6 .

The authors took the explanation of the sponge layers from ECMWF (2016). We shortened the discussion on the sponge layer issue massively. We rather focussed on vertical propagation issues of well-resolved GWs in the troposphere and middle stratosphere during a SSW event. Hence, we decided to not add a discussion on GW parameterization and damping but to quote the Jablonowski and Williamson paper in the introduction.

Orr et al. (2010) discuss the improvements in ECMWF data by changing from Rayleigh Friction to the Scinocca Scheme. Nevertheless, a sponge-specific discussion which would support our statements on resolved GWs in the new manuscript is lacking. Therefore, we dit not include this in our list of references.

As mentioned above, it is simply assumed that the fading of the waves in the upper stratosphere is due to numerical damping alone. However, physical effects and ceasing wind above the polar night jet might be another reason for wave attenuation. Here, wind lidar measurements or the meteor radar winds (see Fig. 2 in Stober et al, 2017) during the SSWs of spring 2016 conducted by colleagues of the home institution of the authors could clarify at least part of the situation during the minor SSWs.

The issues have been discussed in-house before. Our findings found agreements, in general, incuding the intercomparison of unpublished data material. We restrict our method application to a region without massive damping up to the mid-stratosphere and therefore follow the advice of Referee #1 and e.g. Yamashita et al. (2010).

lines 38-42: As far as I know, the pre-processing step of WRF not only interpolates the data on a regular Cartesian grid it also applies some sort of balancing the field to satisfy the WRF equations. There were also scale factors introduced: u and v are multiplied with them to account for the projection used later on. Did this impact the results? Specify exactly which part you have applied to pre-process your data. How was the horizontal divergence calculated? Did you take the ECMWF values or are they calculated by means of WRF-pre-processing? Why was band-pass filtering necessary?

Regarding this concerns, we changed the data preprocessing as described above in Sec. 1. The horizontal divergence is directly taken from ECMWF. Bandpass filter is needed to restrict the analysis on wavelengths that we are intersted in, e.g. intertia gravity waves. Clarification on the sampled GW spectrum can be found in Sec. 2.3 in the new manuscript.

Section 2.4:
- Eq. (13): How is s_delta defined? How is Eq (13) derived? Which assumption went into the derivation? Unfortunately, also the mentioned reference is not very helpful either.

We made it more clearer, now.

Can you give a reference to the statement in line 21?

The relation between amplitude and standard deviation is general for harmonic functions as can be verified with a sine. We added an explanation to Appendix A to show that.

q. (14): I learned that wave action is the mean wave energy (E_KIN+E_POT) divided by the intrinsic frequency, for example Sutherland (2010) Eq. 3.94 or Gill (1982) Eqs. 8.12.33 and 8.6.1.Obviously, Eq. (14) and using "e" as the E_KIN is an approximation. Can you comment why you neglect E_POT?

A derivation of our formulae can be found in Appendix B.

Line 28-31 and PAGE 8 Lines 1-3: you should discuss properties of the wave action and how wave action is changing in s sheared environment!

With this items we want to point out the difference between wave energy and wave action and why we prefere the wave action. A discussion on wave action, especially in varying background winds is part of the discussion, Sec. 4.

3 Results
Section 3.1 The stratospheric conditions in winter 2016 Reading such a headline (I would modify the last part to Arctic winter 2015/16), one would expect that the authors have undertaken a literature research what has already been published about the winter 2015/2016. And there are indeed some articles. Just to mention a few:
Matthias, V., A. Dörnbrack, and G. Stober (2016), The extraordinarily strong and cold polar vortex in the early northern winter 2015/2016, Geophys. Res. Lett., 43, 12,287–12,294, doi:10.1002/2016GL071676.
Manney, G. L. and Lawrence, Z. D.: The major stratospheric final warming in 2016: dispersal of vortex air and termination of Arctic chemical ozone loss, Atmos. Chem. Phys., 16, 15371-15396, https://doi.org/10.5194/acp-16-15371-2016, 2016.
Stober, G., Matthias, V., Jacobi, C., Wilhelm, S., Höffner, J., and Chau, J. L.: Exceptionally strong summer-like zonal wind reversal in the upper mesosphere during win-

ter 2015/16, Ann. Geophys., 35, 711-720, https://doi.org/10.5194/angeo-35-711-2017, 2017.
Dörnbrack, A., S. Gisinger, M.C. Pitts, L.R. Poole, and M. Maturilli, 2017: Multilevel Cloud Structures over Svalbard. Mon. Wea. Rev., 145,1149 159, https://doi.org/10.1175/MWR-D-16-0214.1
All of them deal inter alia with meteorological conditions in the stratosphere, with planetary wave activity, with SSWs, and, eventually, with gravity wave activity in the Arctic. So, they are highly relevant and totally ignored here. As mentioned above, this is not understandable as two of these publications come from the same institutions as the authors themselves.

We have included the named publications in our Introduction.

The section 3.1 is not very focused as it mixes the presentation of meteorological results (mean state in terms of U, Z, gravity waves in terms of DIV, and results from the wave analysis) from the Jan/Feb 2016 period with the discussion. So, a strict separation of presenting results and the discussion is highly recommended to enhance the readability of the text. Furthermore, the comparison to so-called long-term observations in Lindenberg and campaigns in Kühlungsborn is not convincing as the link to SSWs is not obvious. The question stated at the end of line 14, PAGE 9 is either foolish or not necessary as everybody knows that SSWs are large-amplitude PW events deviating the flow from long-term averages.

We seperated Results and Discussion. The comparison with observations from Lindenberg and Kühlungsborn are removed. It was not our aim to sound foolish, so we removed this part, too.

line 8: Are these zonal mean zonal winds plotted in Fig. 3? Clarify this in the text!

This Figure was erased.

line 9: Specify the exact criteria which are used to determine the dates of the minor SSWs? From Fig. 3, there is only information about U.

Not relevant any more.

line 15: What are you referring to? Which "diagnosed GW properties" do you mean? Do you refer to the mean values presented some lines above?

Not relevant any more.

line 17: The first sentence manifests the dilemma of the approach which is followed in the whole Section 3: The authors assume a (I assume local) relation between zonal wind and gravity wave activity without explicitly considering the conditions for excitation and propagation. They selected special geographical locations (60N latitude band, some place near Greenland) and consider the conditions there without taking into account the generation of gravity waves at remote places and their horizontal propagation. At the end, this cumulates in the 1D mechanical analog applying "pumps" and "valves" presented in the final Fig. 9.

In the new manuscript we point out the restrictions on vertical propagation only. We compared our local findings to spatial averages over similiar background wind conditions and found no striking deviations. Therefore, we concentrate on local wave propagation, as it is an advantage of our technique to obtain local wave quantities. Furthermore, we highlight the position of our local GWs.

line 20: there is inconsistency: here and in the Fig. 4 you say: U, Z at 30 km altitude. But how can you plot Z at a fixed altitude? Maybe, the caption is right saying that the plots are at the 10 hPa pressure surface?! Clarify!!

The way how we obtain equidistant height levels from the model levels is described in Sec. 2.1, Step 1. As we use new data now, the polarstereographic maps are redone.

line 21: What "uniformily distributed wind" mean? As the wind consists of a magnitude and direction, a ring vortex can hardly ever have such property.

This is reformulated.

line 22: How do you define the edge of the polar vortex? Which quantitative measure you are using? There is a huge volume of literature devoted to this topic and I'm not *sure what are you referring to.*

The authors are aware of the difficult definition of the edge of the polar vortex. Clearly, this goes beyond the scope of the paper. What is meant is that the bright reader should be capable of combining the wind field (Fig. 2a) with the polar vortex and then sees from the horizontal divergence (Fig. 2b) that anomalies tend to come up at the places where the ring vortex is sharply deformed.

line 23: A sentence like "They are supposed to .." is ridiculous in a scientific paper! There is no proof, no evidence of "typical orographic features", just a statement. Please, go ahead and show that this statement is true. I guess, it will be another full paper. And most probably, you will be forced to modify or revise your statement.

Changed.

lines 23-28, also 32-35: the links to published results should be separated into a discussion chapter and not mixed with the presentation of your results here in this Section 3.

Done.

Generally: the quantification of wave activity is very sloppy although the authors applied a tool to quantify them. Therefore sentences like those in lines 31 ("In this area increased GW activity can be observed in the horizontal divergence field ...") or on PAGE 10,line 2 ("The horizontal divergence field shows much more fluctuations .." should be avoided.

Done

line 4: Avoid statement like this in the presentation of results. They belong to the discussion.

Done.

Section 3.2
PAGE 10,line 7: The logic of the sentence is strange: Why is the focus on "vertical wave propagation since... " the horizontal wavenumber is assumed to be constant?

Changed.

I cannot follow the argument, why a 1D model is sufficient. You only consider conditions at 60N! And from them you conclude later on the mechanisms which are involved. I don't think, this pure mechanistic picture is in any way related to processes in the real atmosphere. There, gravity waves are excited over widespread areas due to a number of sources at different levels from the surface to the mesosphere and they contain a broad spectrum of frequencies and wavelengths. The whole section and the following ones are based on this very strong restriction to assume a wave source near the surface and a pure vertical propagation. I think, this type of argumentation and reasoning is a big step backward from the results on selective wave transmission during SSWs published by Dunkerton and Butchart 33 years ago.

The vertical column modell for GWs is well approved. We are aware that horizontal alignment to strong winds or horizontal propagation play a role but this did not play a leading role by comparing our local profiles to spatial averaged profiles, see discussions above. We now show GWs not only arise from sources from the troposphere, but also from stratospheric jets. We also demonstrate that UWaDi may detect locally very different GW activities in different wind conditions.

PAGE 11
line 4: "westerly orientation": first zonal wind are always east-west winds, so the orientation is clear; second, "westerly" is enough to name wind from the west.

Taken care of.

line 8: in my understanding "wind reversal" means change of sign in U; so, in Fig. 6c I see no reversal at all; the wind must be zero by definition at the surface. Why do you mention this?

This Figure was removed.

Line 10: the comparison of this statement with well-defined wave packets visible at 10 hPa (30 km) in Fig. 4a (divergence) south of the considered band at 60N evidently *show the limited conclusiveness of the analysis. The limited stratospheric wave activity is certainly related to the respective positions with respect to the polar night jet. By the way, this finding is known since years, see the publication of Whiteway et al. (1997) 7 and papers citing his work!*

In the new manuscript we study three different locations at one time step, showing and discussing wind and divergence together with GW parameters. Insofar, we take the relative position with respect to the polar vortex into account. In the Introduction and discussion we mention several more recent publications and their restrictions due to the necessity of spatial or temporal averaging (Yamashita et al., 2010, 2013; Limpasuvan et al., 2011; Ern et al., 2016). We do not claim, that we find results heavily differing from Whiteway (1997) but with this publication we want wo point out the advantages of our method, beneath others we provide snapshots of vertical profiles of local GW propagation without the necessity of e.g. temporal averaging, which was done in Whiteway (1997). We can give local GW properties in faster changing background winds. To keep this manuscript clear, we restricted the list of references to the already listed publications above which support the messsage of our manuscript equally.

On the other hand, such experimental studies could guide you to adapt your analysis strategy to available knowledge.

PAGE 13

Last two paragraphs of Section 3.2: Here, again, you pick a arbitrary location (50W, 60N) and build a 1D model out of it which leads to the left schematic in Fig. 9. This is not to accept as you assume that waves are exited near the surface. First of all, you should show that this is really the case. Second, what frequencies, wavelengths, phase velocities do they have? Third, even assuming that all works out fine for our reasoning: What is so different, so new in your conclusions and in the schematic from the common knowledge about critical level filtering??

The issue of critical level filtering is a good case to show the advantages of the method. Only with a precise estimate for any height the critical level can be identified. Other box-like methods smear out the results, as shown in the test case.

You mention the link to PW activity. Nothing (!!) is shown this respect which gives evidence that the statement is true. Again: what is the progress to the paper of Dunkerton

and Butchart (1984)??
I stop here.

We removed the discussion regarding PWs. The improvements regarding Dunkerton and Butchart (1984) are already discussed above.

FIGURES
Fig 1: Units are missing at the axes. The mentioned crosses are not visible. Or are these the elements of the bold lines?

The figure is redone.

Fig 2: Numbers and units are missing at both of the axes in all panels.

The figure is removed.

Fig 3: It is not clear what exactly is plotted. Zonal mean quantities? Specify! Are the graphs really at 30 km altitude? See Remark to Figure 4 in the text above.

The figure is removed.

Fig 4: Remove the irritating "30 km" label from the figures. It would be helpful not to show the horizontal divergence field alone but also the retrieved wave packets from the algorithm. The scaling of the divergence is too detailed; select a lower absolute value (e.g. 2 10 -4 s -1) for plotting.

The figures are changed according to these comments.

References

Dörnbrack, A., Gisinger, S., Pitts, M. C., Poole, L. R., and Maturilli, M. (2017). Multilevel cloud structures over svalbard. *Monthly Weather Review*, 145(4):1149–1159.

Dörnbrack, A., Pitts, M. C., Poole, L. R., Orsolini, Y. J., Nishii, K., and Nakamura, H. (2012). The 2009-2010 arctic stratospheric winter-general evolution, mountain waves and predictability of an operational weather forecast model. *Atmospheric Chemistry and Physics*, 12(8):3659.

Dunkerton, T. J. and Butchart, N. (1984). Propagation and selective transmission of internal gravity waves in a sudden warming. *Journal of the Atmospheric Sciences*, 41(8):1443–1460.

ECMWF (2016). *Part III: Dynamics and Numerical Procedures*. IFS Documentation. ECMWF.

Ehard, B., Kaifler, B., Dörnbrack, A., Preusse, P., Eckermann, S. D., Bramberger, M., Gisinger, S., Kaifler, N., Liley, B., Wagner, J., et al. (2017). Horizontal propagation of large-amplitude mountain waves into the polar night jet. *Journal of Geophysical Research: Atmospheres*, 122(3):1423–1436.

Ern, M., Thai, Q., John, C., Martin, G., James, M., and Michael, J. (2016). Satellite observations of middle atmosphere gravity wave absolute momentum flux and of its vertical gradient during recent stratospheric warmings. *Atmos. Chem. Phys*, 1680:7324.

Fritts, D. C. and Alexander, M. J. (2003). Gravity wave dynamics and effects in the middle atmosphere. *Reviews of Geophysics*, 41(1). 1003.

Khaykin, S., Hauchecorne, A., Mzé, N., and Keckhut, P. (2015). Seasonal variation of gravity wave activity at midlatitudes from 7 years of cosmic gps and rayleigh lidar temperature observations. *Geophysical Research Letters*, 42(4):1251–1258.

Krisch, I., Preusse, P., Ungermann, J., Dörnbrack, A., Eckermann, S. D., Ern, M., Friedl-Vallon, F., Kaufmann, M., Oelhaf, H., Rapp, M., Strube, C., and Riese, M. (2017). First tomographic observations of gravity waves by the infrared limb imager gloria. *Atmospheric Chemistry and Physics Discussions*, 2017:1–21.

Limpasuvan, V., Alexander, M. J., Orsolini, Y. J., Wu, D. L., Xue, M., Richter, J. H., and Yamashita, C. (2011). Mesoscale simulations of gravity waves during the 2008–2009 major stratospheric sudden warming. *Journal of Geophysical Research: Atmospheres*, 116(D17).

Orr, A., Bechtold, P., Scinocca, J., Ern, M., and Janiskova, M. (2010). Improved middle atmosphere climate and forecasts in the ecmwf model through a nonorographic gravity wave drag parameterization. *Journal of Climate*, 23(22):5905–5926.

Plougonven, R., Teitelbaum, H., and Zeitlin, V. (2003). Inertia gravity wave generation by the tropospheric midlatitude jet as given by the fronts and atlantic storm-track experiment radio soundings. *Journal of Geophysical Research: Atmospheres*, 108(D21). 4686.

Wright, C. J., Hindley, N. P., Hoffmann, L., Alexander, M. J., and Mitchell, N. J. (2017). Exploring gravity wave characteristics in 3-d using a novel s-transform technique: Airs/aqua measurements over the southern andes and drake passage. *Atmospheric Chemistry and Physics*, 17(13):8553.

Yamashita, C., England, S. L., Immel, T. J., and Chang, L. C. (2013). Gravity wave variations during elevated stratopause events using saber observations. *Journal of Geophysical Research: Atmospheres*, 118(11):5287–5303.

Yamashita, C., Liu, H.-L., and Chu, X. (2010). Gravity wave variations during the 2009 stratospheric sudden warming as revealed by ecmwf-t799 and observations. *Geophysical Research Letters*, 37(22). L22806.

Zhao, J., Chu, X., Chen, C., Lu, X., Fong, W., Yu, Z., Michael Jones, R., Roberts, B. R., and Dörnbrack, A. (2017). Lidar observations of stratospheric gravity waves from 2011 to 2015 at mcmurdo (77.84 s, 166.69 e), antarctica: 1. vertical wavelengths, periods, and frequency and vertical wave number spectra. *Journal of Geophysical Research: Atmospheres*, 122(10):5041–5062.

Zimin, A. V., Szunyogh, I., Patil, D., Hunt, B. R., and Ott, E. (2003). Extracting envelopes of Rossby wave packets. *Monthly Weather Review*, 131(5):1011–1017.

Zülicke, C. and Peters, D. (2006). Simulation of inertia-gravity waves in a poleward-breaking Rossby wave. *Journal of the Atmospheric Sciences*, 63(12):3253–3276.

Diagnosis of Local Gravity Wave Properties during a Sudden Stratospheric Warming

Lena Schoon[1] and Christoph Zülicke[1]

[1]Leibniz-Institute of Atmospheric Physics, Schlossstrasse 6, 18225 Kühlungsborn, Germany

Correspondence to: Lena Schoon (schoon@iap-kborn.de)

Abstract. ~~Commonly, wave quantities are maintained in zonal mean averages. Hence, local wave phenomena remain unclear. Here, we introduce a diagnostic tool for studies of wave packets locally. The "Unified Wave Diagnosis" (UWaDi) uses the Hilbert Transform to obtain a complex signal from a real-valued function and estimates the amplitude and wave number locally. Operational data from the European Centre for Medium-Range Weather Forecasts is used to perform the analysis. Restrictions on gravity wave propagation due to model sponge layers are identified well above the 10 hPa altitude. From a minor stratospheric warming in January 2016 three cases for vertical gravity wave propagation in different background wind conditions are selected. It is shown that zonal mean wind quantities cannot reveal local "valves" allowing gravity waves to propagate into the mid-stratosphere. The unexpected finding of high gravity wave activity at the minor warming of 30 January 2016 is related to strong planetary wave activity and a strong local "pump". Accordingly, the advantages of a local wave packet analysis are demonstrated for profiles up to the model sponge layer.~~ The selective transmission of gravity waves through an inhomogenous mean flow is investigated. For the local diagnosis of wave properties we develop, validate and apply a novel method which is based on the Hilbert transform and is named "Unified Wave Diagnostics" (UWaDi). Thus, it provides wave properties at any grid point for any wave-containing data. UWaDi is validated for a synthetic test case comprising two different wave packets. In comparison with other methods, the perfomance of UWaDi is very good with respect to wave properties and their location. For a practical application of UWaDi, a minor sudden stratospheric warming on 30 January 2016 is chosen. Specifying the diagnostics on hydrostatic gravity waves in analyses from the European Centre for Medium-Range Weather Forecasts, we confirm locally different transmission through the middle atmosphere. These are interpreted in terms of columnar vertical propagation using the additionally diagnosed local wave numbers. We also note some hint on local gravity wave generation by the stratospheric jet.

1 Introduction

~~Gravity waves (GWs) have been subject of intense research during the past decades. The scales of GWs reaching from planetary scales (≈ 1000 km) to turbulent microscales (≈ 10m) create a broad field of interest in their role in coupling processes of atmospheric dynamics (Fritts and Alexander, 2003). A phenomenon associated with huge changes in GW appearance is a sudden stratospheric warming (SSW). During a SSW event the middle atmosphere is characterised by three different background wind conditions during a short period of time. Starting with normal winter conditions, followed up by summer-like~~

~~conditions and a slowly transfer back to winder conditions. Respectively, GW variability is associated with changing background wind conditions. Defined by the World Meteorological Organization SSWs are characterised by a reversal of the 60° N to 90° N-temperature gradient. Major warmings are, additionally, associated with a wind reversal at 10 hPa and 60° N, minor SSWs (mSSWs) with a wind deceleration at 10 hPa and 60° N, where the prevailing westerlies are not turned into easterlies. Planetary waves (PWs) play a crucial role in the driving of a SSW event (Andrews et al., 1987). Nevertheless, on the one hand GWs are affected by different background wind conditions that are characteristic during SSWs, on the other hand they are suspected to take, even though a minor, part in the modification of the polar vortex prior to SSWs (Albers and Birner, 2014). Variations in background wind conditions establish zones with wave guides where GWs can propagate easily to higher altitude, as well as forbidden zones of GW propagation (Dunkerton and Butchart, 1984). Models and simulations give the opportunity to analyse the behaviour of GWs and PWs during SSWs up to the mesosphere and lower thermosphere (Liu and Roble, 2002; Limpasuvan et al., 2011, 2012; Hitchcock and Sheperd, 2013; Miller et al., 2013; Albers and Birner, 2014). These studies dealing with GW momentum fluxes are verified by radar measurements (De Wit et al., 2015) as well as satellite observations (Limpasuvan et al., 2011; Yamashita et al., 2013; Thurairajah et al., 2014; Jia et al., 2015; Ern et al., 2016). Ern et al., 2016 point out that the zonal average view of GW parameters that are mainly extracted of models is misleading and local GW activity can vary strongly, especially during SSWs. Next to critical levels, where GWs slow down and eventually dissipate, local regimes of "valves" or "bottlenecks" occur, where the transmission of GWs into the middle stratosphere depends very sensitively on the local wind (Zülicke and Peters, 2008; Kruse et al., 2016). Here we study a minor warming in January 2016 as a test case for local specific propagation conditions for GWs.~~ The importance of gravity waves (GWs) for the dynamics of the Earth's atmosphere is without controversy. They influence dynamics from planetary scales to turbulent microscales and play an important role in the middle atmosphere (Fritts and Alexander, 2003). Here, we want to introduce a new method named "Unified Wave Diagnosis" (UWaDi). The method provides phase-independent local wave quantities like amplitude and wave number without any prior assumption. In the following, we want to develop, validate and apply the novel method. The application concentrates on the analysis of GWs for locally varying background wind conditions in the winter 2015/16.

A common approach to obtain vertical wave numbers and GW frequency of high-passed filtered wind fluctuations are Stokes parameters (Vincent and Fritts, 1987). This method is based on the definition of polarisation relations and works for single-column measurements. It provides the wave properties in preselected vertical height sections of finite lengths. Next to its original application on radar measurements it is used for radiosonde data (Kramer et al., 2015). A supplement to this method named DIV was introduced by Zülicke and Peters (2006). It determines the dominating harmonic wave in a box from the first zero-crossing of the auto-correlation function. The maximal dectectable wavelength is restricted by the box size. The analysed quantity is the horizontal divergence to get the ageostrophic flow without numerical filtering. A further technique is based on sinusoidal few wave fits (S-3D) (Lehmann et al., 2012). This method was created for the analysis of binned data from remote sensing (Ern and Preusse, 2012; Ern et al., 2014, 2017; Krisch et al., 2017) but is also applicable to model data (Preusse et al., 2014). The first two modes with highest variance are taken from a fit that minimises the variance-weighted squared deviations over all points in a box. Only a small number of sinusoidal curves are fitted and there might remain uncovered variances in the analysis volume. All these methods have in common, that the analysed spatial scales are dependent on the predefined analysis box size and the assumption of spatial homogeneity of the wave field in these boxes. Nevertheless, these methods are superior to a classic Fourier transform in that point that they allow to search for waves with bigger wavelengths than the box size. Here, we want to develop a method which provides wave parameters locally, meaning at each grid point.

Another three-dimensional spectral analysis method is the 3-D Stockwell-transform (3D-ST) (Wright et al., 2017). This method is capable of analysing the full range of length scales sampled in satellite data and is not restricted to box sizes. At every grid point, a local wave spectrum is estimated. With this method available local wave quantities are wavevectors, amplitudes, phase and group velocities, temporal frequencies and momentum fluxes. However, directions of vector quantities have to be fixed by seperate assumptions. Both, S-3D and 3D-ST look for the largest spectral amplitude to calculate the wave quantity at the respective box point. This might lead to a loss of information, in any case the estimated variance is too small. We search for a method which detects the full variance in each data point.

With UWaDi we find the dominating wave with the Hilbert transform. It makes data binning into boxes redundant and is developed to work with equally-gridded data. In general, the Hilbert transform can be applied to data of any dimensionality. Wave properties such as the amplitude are estimated phase-independently. Every variable including any kind of wave-like structure is analysable and preselection of modes is avoided. Zimin et al. (2003) used the method to obtain the envelope of a train of Rossby waves in one dimension. A supplement was made for waves not in-line with grids by an extension of the formulation to stream lines to obtain quasi-one-dimensional wave packets (Zimin et al., 2006). Kinoshita and Sato (2013) provide a three-dimensional application on Rossby and GWs. Our method comes up with an enhancement for three dimensions and the additionally provision of the wave number in every dimension which was not presented before. We aim to cover the retrieval of local wave properties from arbitrary orientated wave packets. Amplitude and wave number are sampled on the same grid as the input data. After the mathematical description of the method it will be validated with synthetic datasets to demonstrate its quality in comparison with other methods.

For a practical application in geophysical context, we will investigate GWs. Their sources are usually found in the troposphere where waves are generated by flow over orography, convection, frontal systems and jet imbalances. These waves propagate upwards with increasing amplitudes and break in the middle atmosphere where they deposit their momentum to the background flow. Strong influence is exerted on global circulation patterns in the mesosphere as well as in the stratosphere (Holton, 1983; Garcia and Salomon, 1985)). GWs play crucial roles in the modulating of the quasi-biennial oscillation (QBO) and the Brewer-Dobson circulation (Dunkerton, 1997; Alexander and Vincent, 2000; Ern et al., 2014). Another stratospheric phenomenon where GWs play a role are sudden stratospheric warmings (SSW). A variety of definitions exists (Butler et al., 2015), but the most common one is given by the World Meteorological Organization stating that a SSW is characterised by a reversal of the 60° N to 90° N-temperature gradient. Major warmings are associated with a wind reversal at 10 hPa and 60° N; minor SSWs (mSSWs) with a wind deceleration at 10 hPa and 60° N, where the prevailing westerlies are not turned into easterlies. Even though planetary waves are the most important drivers of SSWs (Andrews et al., 1987), GWs are affected by the differing background wind conditions during SSWs and are suspected to modulate the polar vortex in the postwarming phase of a SSW (Albers and Birner, 2014). The coupling of GWs with planetary waves during a SSW was investigated by simulations and different measurement techniques. Restricted to zonal mean wave properties, local eastward propagating GWs can only be estimated by anomalies in horizontal divergence fields. Nonetheless, these GWs are, next to selective transmission, assigned to GW emission and unbalanced flow adjustment (Yamashita et al., 2010; Limpasuvan et al., 2011). We are interested in the longitude-dependent transmission of GWs during a SSW. Pioneering work was done by Dunkerton and Butchart (1984). They analysed model data and found that selective transmission of GWs during a SSW is dependent on longitude. Therefore, regions where vertical wave propagation is inhibited exist as well as regions where waves can propagate up to the mesosphere. The analysis of Dunkerton and Butchart (1984) was restricted to parameterized GWs of the “intermediate range”, that they defined between 50 km and 200 km. They state that it remains unclear, in what kind GWs of larger scale will act during SSWs. A study on a self-generated SSW in a model showed that GWs reverse the circulation in the mesosphere-lower thermosphere during a SSW by altering the altitude of GW breaking. This altitude is highly dependent on the specification of GW momentum flux in the lower atmosphere (Liu and Roble, 2002). This is where our analysis sets in. We want to diagnose the appearance of GWs precisely in space and give an interpretation using the information on their changing amplitude and wave number. For that purpose, we will use UWaDi with a GW-specific diagnostic.

The northern winter 2015/16 brought up several interesting features, including several issues of GW behaviour. The beginning of the winter was characterised by an extraordinarily strong and cold polar vortex driven by a deceleration of planetary waves in November/December 2015 (Matthias et al., 2016). Thereinafter, for the end of that winter a record Arctic ozone loss was expected (Manney and Lawrence., 2016). Furthermore, the extraordinarily polar vortex caused a southward shift of planetary waves leading to anomalies in the QBO (Coy et al., 2017). Inbetween, a joint field campaign of the research projects METROSI, GW-LCYCLE 2 and PACOG took place in Scandinavia in January 2016. Stober et al. (2017) found a summer-like zonal wind reversal in the upper mesosphere lasting until the end of January 2016, leading to different GW filtering processes in the mesosphere compared to usual winter-like wind conditions. During the field campaign first tomographic observations of GWs by an infrared limb imager provide a full three-dimensional picture of a GW packet above Iceland (Krisch et al., 2017). Additionally, a remarkable comparative study shows that forecasts of the current operational cycle (41r2) of the European Centre for Medium-Range Weather Forecasts (ECMWF) Integrated Forecast System (IFS) shows good accordance with space-borne lidar measurements while picturing large-scale and mesoscale wave structures in polar stratospheric clouds (Dörnbrack et al., 2017). We choose the mid-winter of 2016 for an application of UWaDi because it is very well sampled with observations of GW properties. Hopefully, we may provide additional impulses to the evaluation of observations.

~~Assimilated data products from the European Centre for Medium-Range Weather Forecasts (ECMWF) are suitable to analyse local phenomena and their coupling, as they resolve essential parts of GW dynamics in the stratosphere, sufficiently. The T799 resolution already gives proof of correct GW appearance in the stratosphere. Validation with satellite measurements point out that ECMWF GWs from the tropics are not realistic (Preusse et al., 2014), but mid- and high-latitude GWs are captured well by ECMWF analysis (Yamashita et al., 2010). The recently introduced and improved T1279 resolution yields to a bigger portion of resolved GWs in ECWMF data. Even though the tropical portion of parameterised convective GWs is still too small, mid-latitude GWs are captured well being driven by orographic and jet-stream associated sources (Shutts and Vosper, 2011). A comparison with balloon-borne measurements on the southern hemisphere shows an underestimation of momentum fluxes by the factor of 5 of ECMWF GWs in mid-latitudes but the overall appearance and propagation of GWs are realistic (Jewtoukoff et~~

~~al., 2015). Hence, ECMWF resolved GWs meet our requirements to identify local valves. In particular, we want to investigate local quantities of resolved GWs in the ECMWF analysis for different background wind conditions. In order to perform such an analysis, the GW amplitudes and wave numbers need to be locally diagnosed in three dimensions.~~

~~Another issue is the search for varying GW sources because there is some likeliness that strong PWs govern jet streaks. From their exit regions GWs may be radiated by spontaneous imbalance which may "pump" them into the middle atmosphere (Uccelini and Koch, 1987; O'Sullivan and Dunkerton, 1995; Pluogonven et al., 2003). Several methods to extract wave properties can be found in literature. Most of these methods are linked to a limited range of wave frequencies and/or special observation techniques. Hence, most of these methods provide wave properties by spatial averaging and therefore accept a loss of information. Starting with the analysis of PWs, two-dimensional zonal-mean effects can be described by the Eliassen-Palm flux (Andrews et al., 1987). Extended studies on three-dimensional wave propagation yield to the wave activity flux (WAF) (Plumb, 1985, 1986) with an analogue for GWs, the gravity wave flux (Bretherton, 1966). The unification of these fluxes lead to a three-dimensional WAF describing wave propagation both for inertia GWs and PWs (Kinoshita and Sato, 2013a). Further studies provide corrections for more accurate magnitudes and directions of wave propagation (Kinoshita and Sato, 2013b) as well as a separate formulation for equatorial waves (Kinoshita and Sato, 2014). While these approaches are designed to estimate the pseudo-momentum flux, a more kinetically oriented approach asks for wave amplitudes and wave numbers. A common approach to obtain vertical wave numbers and GW frequency of high-passed filtered data are Stokes parameters (Vincent and Fritts, 1987). This method works for single vertical measurements and provides the wave properties in several vertical height sections. Another method that is capable to derive wave numbers in all three dimensions uses auto-covariance functions defined over spatial-averaged boxes (Zülicke and Peters, 2006). Therein, it is utilised that the use of the horizontal divergence simplifies the harmonic analysis by neglecting geostrophic flow by definition and redundantises filtering processes. Local wave properties are obtained by an one-dimensional signal-processing technique named the Hilbert Transform. Zimin et al. (2003) introduce the method by providing the amplitude of a wave packet for an arbitrary set of waves. Rewriting the formulation to work on streamlines makes it more adaptable to various quasi one-dimensional propagations of wave packets (Zimin etz al., 2006). An adaption to Rossby wave trains shows good results and recommends this approach (Glatt and Wirth, 2014). Furthermore, it is generalised for different directions addressing multi-dimensional problems by Kinoshita and Sato (2013).~~

In particular, UWaDi requires regular gridded data. Assimilated data products from ECMWF are suitable to analyse local phenomena and their coupling as they resolve essential parts of GW dynamics in the stratosphere. Even the T799 resolution gives proof of correct GW appearance in the stratosphere. Validation with satellite measurements point out that ECMWF captures GWs well in the mid- and high-latitudes (Yamashita et al., 2010; Preusse et al., 2014). The improved T1279 resolution yields to a bigger portion of resolved GWs in ECMWF data. Validation studies with measurements show that mid-latitude GWs are captured well being driven by orographic and jet-stream associated sources (Shutts and Vosper, 2011; Jewtoukoff et al., 2015). Our approach concentrates on fields of horizontal divergence of ECMWF IFS data. The horizontal divergence counts for a dynamical indicator for GWs (Plougonven et al., 2003; Zülicke and Peters, 2006). Its magnitude was found to correlate with temperature anomalies induced by mountain waves (Dörnbrack et al., 2012; Khaykin et al., 2015). We concentrate on vertical propagation only, highlighting selective transmission. Studies arguing the restrictions on vertical-only propagation can be found in Yamashita et al. (2013), Kalisch et al. (2014) and Ehard et al. (2017). We point out that meridional propagation of GWs can play an important role for the analysis of the deposition of GW drag in the mesosphere. As we give an idea of GW propagation in the upper troposphere and stratosphere we concentrate on vertical propagation and are aware of the possibility of GW entrainment of strong winds.

~~With this paper we introduce a new method to obtain phase-independent wave properties locally. The vertical propagation of GWs during different background wind conditions induced by a mSSW serves as an example to detect local valves in vertical GW transmission. ECMWF reanalysis data are chosen to meet our requirements. The paper is organised as follows. After providing an overview of the newly developed method to obtain wave properties locally in Sect. 2, two synthetic examples of wave packets are given to validate and demonstrate the advantages of the new algorithm. This section is followed by a description of the used ECMWF data and the wave quantities needed for the analysis of GW properties during a SSW. In Sect. 3 three time phases around a mSSWs in January 2016 are investigated for valves of vertical wave transmissions: the prewarming, midwarming and postwarming phase. A summary, discussion and outlook are found in Sect. 4.~~ The paper is organised as follows. After providing a step-by-step introduction and validation of the novel method in Section 2, we give a short overview of the estimation of wave quantities for synthetic data and describe the analysis data. In Section 3 we show our results for the mSSW on 30 January 2016 where we study local GW generation and propagation. The discussion of our results in Section 4 is followed by the Summary and Conclusion (Sec. 5).

2 Method and data

~~Hereafter, we develop and validate an algorithm to extract wave parameters from an equidistant three-dimensional data. It reads, processes and plots autonomously, accepting user-defined flags in an attached namelist. For local diagnosis of waves, e.g. inertia gravity waves, phase-independent estimates are essential. Therefore, complex quantities are constructed for an amplitude-phase presentation by a Hilbert Transform (Von Storch and Zwiers, 2001; Zimin et al., 2003, Sato et al., 2013). Additionally, wave numbers are estimated. We call this procedure "Unified Wave Diagnosis" (UWaDi). The method is sketched briefly.~~ In this section we develop and validate an algorithm to extract wave parameters from three-dimensional data. For local diagnosis of waves, phase-independent estimates of wave amplitudes as well as the wave vector are essential. For this, we employ the Hilbert transform (Von Storch and Zwiers, 2001). The Hilbert transform shifts any sinusoidal wave structure by a quarter phase, i.e. turning a sine into a cosine. By constructing a new complex number consisting of the original field as real part and its Hilbert transform as the imaginary part, the absolute value is always the amplitude (square root of squared real and imaginary part). The amplitude is independent of the phase and the wavelength of the oscillation and there is no need of any explicit fitting of a wave. In addition, the absolute wave number in all three dimensions is determined from the phase gradient.

2.1 Step-by-step outline of the method

~~Complex values of a function $f[x]$ are found with the Hilbert Transform in x-direction:~~

$$\hat{f}[x] = f[x] + iH(f[x]).$$

~~The Hilbert Transform provides a new complex series $\hat{f}[x]$ compounded of the sum of the original function $f[x]$ as the real part and the Hilbert-transformed series $H(f[x])$ as the imaginary part. Literally, the Hilbert Transform shifts $f[x]$ a quarter to the right $(-\frac{\pi}{2})$ turning a cosine into a sine and a sine into a minus cosine.~~

~~The Hilbert Transform itself is composed of three steps (Zimin et al., 2003). First, a discrete Fourier Transform (DFT) is conducted~~

$$[k] = \mathrm{DFT}(f[x]),$$

~~followed by an user-defined bandpass filtering process $(0 < k_{min} < k_{max})$~~

$$f_{filtered}[k] = F(k_{min}, k_{max})f[k],$$

~~and an inverse DFT~~

$$\hat{f}[x] = 2 * \mathrm{DFT}^{-1}(f_{filtered}[k]).$$

~~Using this complex series, we estimate the amplitude and wave number of a wave packet.~~
~~The amplitude is maintained by (Schönwiese, 2013)~~

$$a[x] = |\hat{f}[x]| = \sqrt{f[x]^2 + H(f[x])^2}$$

~~and gives an estimate of the local envelope of an oscillating function.~~
~~The phase Φ~~

$$\Phi[x] = \mathrm{atan}\left(\frac{H(f[x])}{f[x]}\right)$$

~~is used to derive the absolute wave number~~

$$k_x[x] = \frac{d\Phi[x]}{dx}.$$

~~By highlighting the use of UWaDi for three-dimensional data the wave number-weighted three-dimensional quantities are the main gain~~

$$a_{final}[x,y,z] = \sqrt{\frac{\sum_d q_d k_d^2 a_d^2}{\sum_d q_d k_d^2}}$$

~~and~~

$$k_{final}[x,y,z] = \sqrt{\sum_d q_d * k_d^2}$$

~~with $d = [x,y,z]$. By using this method, wave properties for every dimension d are obtained separately and get combined in the last step of the algorithm to a three-dimensional field of local wave properties. q denotes the quality flag. Included are different quality checks. Fist, the amplitude and wave number are checked for at least a half undamped wave considering the packet length l ($k \times l > \pi$). Second, noise suppression is considered by taking into account the standard deviation of the data and creating a threshold under which results are rejected (Glatt and Wirth, 2014). Third, high frequency fluctuations in amplitude and wave number are smoothed by a running mean over a number of grid points, respecting the minimum wave number k_{min} of the bandpass filter.~~

~~This method does not cover the temporal propagation of a wave packet and therefore the wave number misses sign ($k = \pm k[x]$).~~ In the following we introduce UWaDi by a step-by-step outline. Further, we validate it with a well-defined test wave packet in comparison with other methods. In general, UWaDi is a script package which allows the user to steer data preprocessing, the main wave analysis and data plotting, from a set of namelists. This package is coded in open source software such as NCL and Fortran. Its multi-purpose applicability on a set of arbitrary waves, e.g. gravity waves or planetary waves, defines its unified character.

1. Firstly, the three-dimensional gridded data is preprocessed. UWaDi requires data from equidistant grids. Horizontally, the grids are equidistant if they are provided on a regular latitude-longitude grid. The latitude-dependence of grid distance is taken into account. Vertical interpolation from model levels to equidistant height levels is performed by associating constant heights with pressure levels. This might cause problems in areas of high orography and inside the planetary boundary layer. Both are avoided in the following application. Consider to first separate the fluctuations from the background with appropiate numerical or dynamical filters.

2. The underlying Hilbert transform starts with a Discrete Fourier Transform (DFT) which creates a complex series in wave number space f_k from the real valued data f_x (e.g. Smith et al. (1997)):

$$f_k = \mathrm{DFT}(f_x) \tag{1}$$

3. DFTs can be biased by variance leakage through side lobes in spectral space. Tapering methods abandon this but can smear out nearby wave numbers. A loss of absolute amplitude can be overcome by using normalised weights (Von Storch and Zwiers, 2001). For the present study, however, the best results were obtained by turning the taper off.

4. In wave number space a rectangular bandpass filter reduces the complex series to the user-predefined wave number limits k_{min} and k_{max}. Here, we make sure that only waves of the considered range of wave numbers are used for the following

analysis.

$$f_{k,filtered} = F(k_{min}, k_{max}) f_k, \tag{2}$$

5. To get back from wave number space an inverse DFT is performed.

$$\hat{f}_x = 2 * \mathrm{DFT}^{-1}(f_{k,filtered}). \tag{3}$$

6. The such constructed complex valued function $\hat{f}_x$ of the input data f_x as the real part and the Hilbert-transformed function $H(f_x)$ as the imaginary part

$$\hat{f}_x = f_x + iH(f_x) \tag{4}$$

provides the amplitude a_x (Schönwiese, 2013)

$$a_x = |\hat{f}_x| = \sqrt{{f_x}^2 + H(f_x)^2} \tag{5}$$

and the phase estimate Φ_x

$$\Phi_x = \mathrm{atan}\left(\frac{H(f_x)}{f_x}\right). \tag{6}$$

7. The phase gradient is a measure of wave number

$$k_x = \frac{d\Phi_x}{dx} \approx \frac{\left|\mathrm{DFT}^{-1}(k\mathrm{DFT}\hat{f}_x)\right|}{|\hat{f}_x|}. \tag{7}$$

8. Due to the finite character of the data series it may happen that high-frequency fluctuations appear after the Hilbert transform. We neglect those by applying a low-pass filter. We smooth over a number of grid points determined by the lower wave number limit k_{min}.

9. Alienation of outliers is taken care of by two different quality. Firstly, the amplitude and wave number are checked for at least a half undamped wave. Therefore, the packet length l_x is essential. It is calculated by covariance functions C_{xx}:

$$l_x = \sum_{x=0}^{x_{max}} \left|\frac{C_{xx}}{C_{00}}\right| \tag{8}$$

with $x_{max} = \frac{N-1}{5}$ (Chatfield, 2016). This method goes back to Zülicke and Peters (2006). The quality check then is defined by the inequality

$$k_x l_x > \pi. \tag{9}$$

Secondly, the retrieved signals are supposed to lie above the noise level of the input data. An empirical threshold c checks the amplitude for being valid considering the standard deviation of the input horizontal divergence δ

$$a_x > c * \delta(f_x). \tag{10}$$

Empirically, we use $c = 0.01$. This idea follows Glatt and Wirth (2014).

UWaDi uses a quality flag $q = 1$ which is set to false ($q = 0$) if at least one quality check is rejected.

10. Steps 2 to 7 are repeated for the other dimensions (y,z).

11. Amplitude and absolute wave number are saved on the same grid as the input data to create a full three-dimensional analysis of local wave quantities. The amplitude is combined to a wave number-weighted sum of the three spatial dimensions

$$a_{(x,y,z)} = \left(\frac{\sum_{d=x,y,z} q_d k_d^2 a_d^2}{\sum_{d=x,y,z} q_d k_d^2} \right)^{\frac{1}{2}}. \tag{11}$$

The absolute wave number is determined by

$$k_{(x,y,z)} = \left(\sum_{d=x,y,z} q_d * k_d^2 \right)^{\frac{1}{2}}, \tag{12}$$

with d denoting the spatial index.

The method provides an exact measure of the amplitude in the sense of the sum of squared amplitudes of the wave modes. The dominating wave number is the amplitude weighted sum of all. Spectrally wide dynamics can cause a significant reduction of information (Appendix A). Applying UWaDi with several narrow band-pass limits would provide information on spectrally spread waves. However, the method is recommended for the first guess of the dominant wave packet.

~~**Analytical test case**~~

2.2 Validation of the method

~~Synthetical one- and two-dimensional test cases are considered to proof the reliability of UWaDi.~~

~~**One-dimensional wave packet**~~

~~An one-dimensional example is adapted from Zimin et al. (2003). Two consecutive wave packets with the wave numbers 4 and 9 are given by~~ For a comparison of available methods that obtain wave quantities we choose the test case presented in Zimin et al. (2003) (Fig. 2a). A couple of localized wave packets with the wave numbers 4 and 9 is given in one dimension on the interval $[0,4\pi]$ by

$$f[x] = \exp\left[-(x-4.5)^2\right]\cos(4x) + \exp\left[-(x-7.5)^2\right]\cos(9x). \tag{13}$$

~~UWaDi is performed for bandpass limits of wave numbers of 1 and 10. The amplitude peaks with 1.0 and envelopes the consecutive wave packets well (Fig. 1). Crosses mark the calculations passing the quality checks. The red lines show the threshold under which calculated values are treated as noise. This threshold can be chosen by the user to suit the individual~~

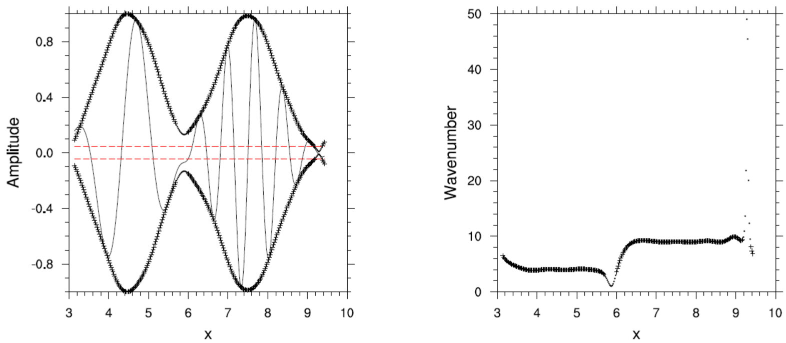

Figure 1. ~~One-dimensional test function (bold line, left figure) adapted from Zimin et al. (2003). UWaDi-calculated amplitude enveloping the test function (left) with crosses marking valid values according to the quality check. Additionally, the red lines specify thresholds belonging to the quality check which suppresses noisy signals. The calculated wave number (right) uses the same markers.~~

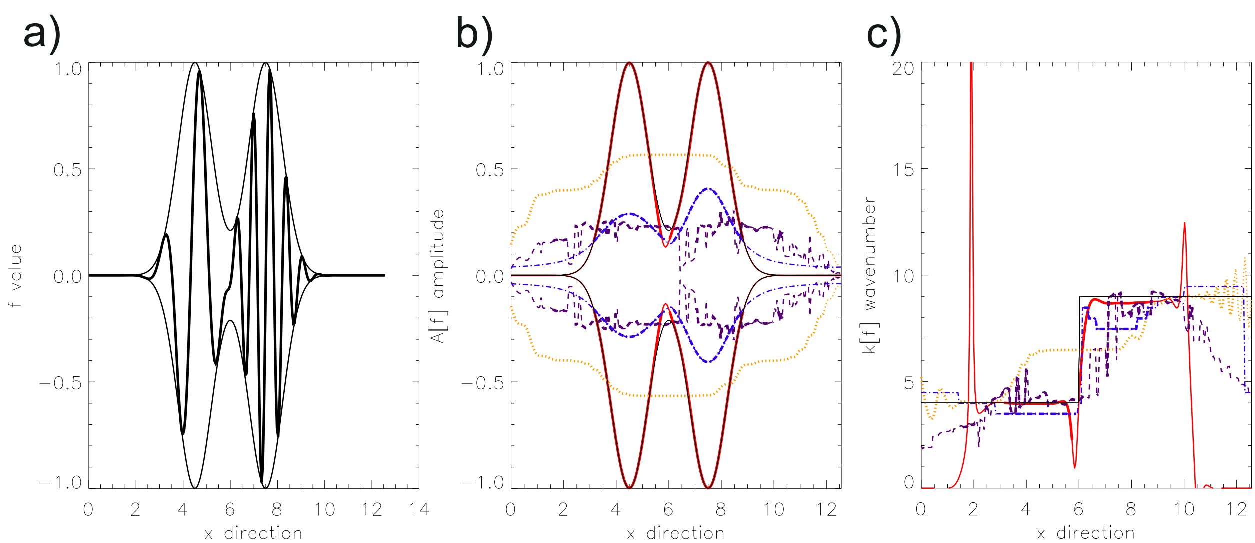

Figure 2. One-dimensional test function (bold line, left figure) adapted from Zimin et al. (2003) and its envelope. Comparison of amplitude (centre) and wave number (right) calculated by different methods: UWaDi (solid, red), DIV (dotted, orange), S-3D (dashed, violet) and 3D-ST (dash-dotted, blue). Valid estimates are drawn in bold.

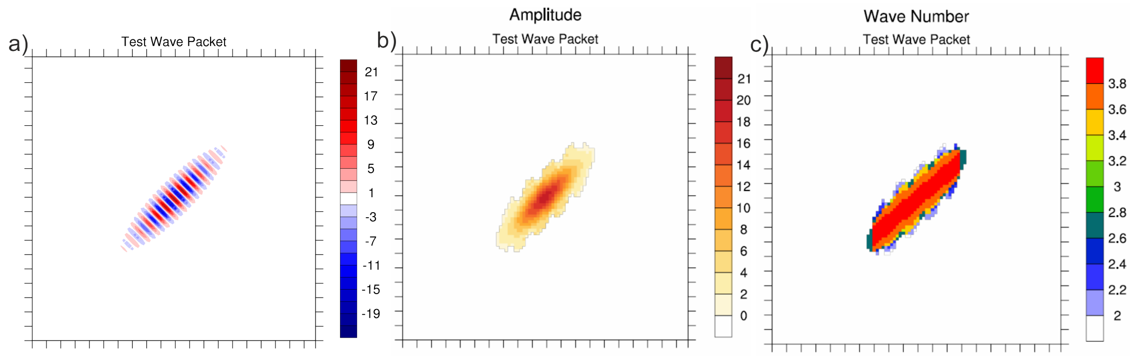

Figure 3. ~~Two-dimensional test wave packet. a) Test wave packet according to Equation 14. b) Amplitude calculated by UWaDi and c) wave number in two-dimensional combination by UWaDi.~~

~~problem. A small gap in valid amplitude values occurs at the transition between both wave packets, helping the user to distinguish between several wave packets in the analysis. The wave number shows fluctuations in areas where the amplitude becomes small. These are artefacts from the DFT and not considered as they do not pass the quality checks. We admit that the calculation of wave number is less unique but the wave numbers 4 and 9 are distinguishable. Hence, the method performs well in regions with sufficiently large amplitudes of the carrier waves.~~

Here, the quality check (step 9) requires the amplitudes to exceed half of the sample standard deviation.

The method showing the best agreement with the theoretical value is UWaDi (Fig. 1b). For the amplitude both wave packets are clearly distinguishable and the maximum peaks are recovered exactly. As expected, the 3D-ST method shows a rebuilding of the wave packet's shape as well. The lack of absolute amplitude value might be overcome with empirical correction factors Nevertheless, the amplitudes of both wave packets differ from each other. A higher peak of amplitude is given by the DIV method but the two wave packets are smeared out. A similar pattern is shown for the S-3D method. Both latter methods show high dependence on the chosen box size withing the analysis. The wave number calculation is best for UWaDi (Fig. 1c). The high peaks at the beginning and end of the wave packets are sorted out by the quality check. S-3D and 3D-ST show good results in peaking at the right value but do not cover the complete spatial range of the wave packet. Wave number calculation of DIV shows higher deviations. Altogether, UWaDi shows nearly perfect agreement with the theoretical expectations.

~~**Two-dimensional wave packet**~~

~~A two-dimensional wave packet is given by~~

$$f[x,z] = a\exp\left(-\left(\frac{z'^2}{l_z'^2}+\frac{x'^2}{l_x'^2}\right)\right)\cos\left(k_z z' + k_x x'\right) \quad (14)$$

~~with an adapted coordinate system that might be rotated by α~~

$x' = x\cos(\alpha) + z\sin(\alpha),\ z' = -x\sin(\alpha) + z\cos(\alpha).$

~~For this study following parameters are chosen:~~

$$l'_x = 4,\; l'_z = 1,\; a = 21,\; k_x = 4,\; k_z = 0,\; \alpha = \frac{\pi}{4}.$$

~~Figure 3a shows the wave packet build by Equation 14.~~

~~The amplitude peaks with 21 (Fig. 3b) and the wave number with 3.8 (Fig. 3c). The edges of the wave packets in amplitude and wave number are not sharply contoured and show decreases of values to the edge, which is due to the small amplitude of the wave packet to its boundaries, as previously reported. Hence, the amplitude is captured well and the wave number estimation differs just slightly (about 5 %) from the input value.~~

~~The one- and two-dimensional wave packets had been further analysed in different noisy backgrounds and for several tilts. Effects on amplitude and wave number are negligible. Furthermore, one can envision that UWaDi may underestimate wave packets at the boundaries of the input field due to finite data strings in the DFT. Indeed, as long as the wave packet is one wavelength away from the field boundaries, UWaDi gives reliable results.~~

2.3 Analysis Data

~~ECMWF data from the Integrated Forecasting System (IFS) is chosen for this analysis. The IFS builds the base for the forecasts of ECMWF. The chosen data set has the spectral resolution T1279 ($0.125° \times 0.125°$ longitude-latitude grid, ca. 16 km grid spacing) and L137 (number of model levels, reaching up to ca. 80 km altitude). The temporal resolution is 6 hours. Recent studies showed that ECMWF IFS data captures seasonal and geographical GW variability up to the lower stratosphere in mid- and high-latitudes (Wu and Eckermann, 2008; Yamashita et al., 2010; Shutts and Vosper, 2011; Preusse et al., 2014; Jewtoukoff et al., 2015).~~

~~Vertical propagating GWs are damped in ECMWF IFS products from 10 hPa (≈30 km) upwards (ECMWF, 2016). At 10 hPa the stratospheric sponge starts and a damping of wave propagation is expected. The mesospheric sponge follows at 1 hPa acting on the divergence and therefore directly on the GW properties.~~

~~For this analysis the primary T1279 resolution is restricted to an $1° \times 1°$ longitude-latitude grid to resolve mesoscale GWs (≈200 to 2000 km). The sampling theorem indicating that signals above the length of two times the grid space are captured, therefore allows for a detection of 222 km horizontal wavelength. The vertical level spacing in the stratosphere is about 1 km, which allows for a presentation of 2 km vertical wavelength in this analysis.~~

~~UWaDi requires an equidistant grid in all three dimensions. To overcome this issue, the Weather and Research Forecasting (WRF) Preprocessing System (WPS) is used. It is a tool to convert a model grid to an equidistant grid (cartesian coordinate system) (Skamarock et al., 2008). In order to select GW-relevant scales, we band-passed for a longitudinal set of wavelength between $\lambda_x = [300\text{km} \ldots 1500\text{km}]$, the meridional range of wavelength is chosen to be $\lambda_y = [700\text{km} \ldots 3000\text{km}]$ and for the vertical GWs we set the limits to $\lambda_z = [1\text{km} \ldots 15\text{km}]$.~~

ECMWF data from the IFS operational cycle 41r1 is chosen for this analysis. Together with the latest cycle 41r2 it is based on T1279 L137 but differs in its effective horizontal resolution and non-orographic gravity wave parameterization. Cy41r2 reduces the distance between grid points to 9 km, from former 16 km. Not shown comparison studies between IFS data provided on different grid sizes ($0.1°, 0.36°, 1°$) considering our bandpass filter conditions gave reliable and comparable results for the $0.1°$- and $0.36°$-grids. Therefore, we decide that the former cycle stored with a resolution of $0.36°$ (ca. 40 km) meets our requirements. We discuss resolved gravity waves of a horizontal scale between 100 km and 1500 km. In vertical direction we are interested in gravity waves within the wave length limits of 1 km to 15 km. These scales fullfill the assumption of hydrostatics and cover the range of mid- and low-frequency GWs (Guest et al., 2000).

Vertical propagating GWs are damped in ECMWF IFS products from 10 hPa (≈30 km) upwards (ECMWGF, 2016). At 10 hPa the stratospheric sponge starts and a damping of wave propagation is expected (Jablonowski and Williamson, 2011). The mesospheric sponge follows at 1 hPa acting on the divergence and therefore directly on the GW properties. We restrict our analysis to a maxmimum altitude of 45 km and therefore follow the advice of Yamashita et al. (2010). The regular latitude-longitude grid is remained during the analysis. We interpolate model levels to equidistant height levels between 2 km to 45 km with a distance of 500 m.

~~Wave quantities~~

2.4 Gravity-wave specific quantities

~~We choose the horizontal velocity divergence $\left(\delta = \frac{\partial u}{\partial x} + \frac{\partial v}{\partial y}\right)$ as the target quantity. By this, we operate on ageostrophic fields which contain essential parts of GW fluctuations without applying any numerical filtering procedure to separate wave and mean flow (Zülicke and Peters, 2006). From the diagnosis of this field, the amplitude (a) and the wave numbers (k_x, k_y, k_z) are obtained.~~

~~The kinematic wave energy (that is energy per mass, in units $\left[\mathrm{m^2 s^{-2}}\right]$) is derived from polarisation equations assuming hydrostatics (Zülicke and Peters, 2006)~~

From the diagnosed fields of amplitude and wave number we calculate the kinematic wave energy e and wave action A. In order to find the ageostrophic GW motion we analyse fields of horizontal divergence. The kinematic wave energy is derived from polarisation equations for GWs assuming hydrostatics (Zülicke and Peters, 2006) (Appendix B):

$$e = \frac{s_\delta^2}{k_h^2} = \frac{a^2}{2}\frac{1}{k_x^2 + k_y^2}, \tag{15}$$

~~presuming the definition of signal processing techniques that the variance is expressible of terms of the amplitude: $s^2 = \frac{a^2}{2}$.~~
In this formula we need information on the variance and the horizontal wave number. Both are provided by UWaDi.

$$\delta^2 = \frac{a^2}{2} \tag{16}$$

$$k_h^2 = k_x^2 + k_y^2 \tag{17}$$

The wave action is a conserved quantity describing waves in the presence of an imhogeneous background wind ~~but not interacting with the mean flow~~ (Bretherton, 1966). It does not change for upward propagating wave as long as they do not interact with the mean flow. The wave action is defined by putting the kinematic wave energy e in relation to the intrinsic flow-relative frequency $\cancel{\Omega}$ ω:

$$A=\rho\frac{e}{\Omega},A=\rho\frac{e}{\omega}, \tag{18}$$

ρ being the density. The intrinsic frequency $\cancel{\Omega}$ ω is calculated by the dispersion relation in mid- and low-frequency approximation: $\cancel{\Omega^2=f^2+\frac{N^2\left(k_x^2+k_y^2\right)}{k_z^2}}$ $\omega^2=f^2+\frac{N^2\left(k_x^2+k_y^2\right)}{k_z^2}$.

~~Say~~ From $\cancel{A=\rho\frac{e}{\Omega}=\text{constant}}$ $A=\rho\frac{e}{\omega}=\text{constant}$, one can see the following

- density effect: $e\propto\frac{1}{\rho}\propto\exp\left(\frac{z}{H}\right)$. The above derived energy undergoes an exponential increase according to the density with the scale height H in vertical direction z.

- wind effect: $\cancel{e\propto\Omega}$ $e\propto\omega$. From the apparent phase speed $\cancel{c=\frac{\Omega}{k}+u}$ $c=\frac{\omega}{k}+u$ one gets the dependence of the intrinsic frequency: $\cancel{\Omega=k(c-u)}$ $\omega=k(c-u)$. Assuming constant phase speed c and a constant wave number k for a wave packet, meaning that a wave is propagating in a horizontally homogenous wind $u(z)$, one has to accept that the energy scales with the background wind u.

~~Hence, wave action is used primarily for the following analysis. The effect of density and wind on the profiles of wave energy is discussed for selected examples.~~ For the following analysis primarily wave action is used.

3 Results

3.1 The stratospheric conditions in winter 2016

~~A period of interesting wind features during winter 2016 is chosen to be 21 January to 21 February 2016. Figure 4 shows the zonal wind in green at an altitude of 30 km and 60° N. This time series is characterised by strong wind fluctuations. Notable features are the high wind speeds at the beginning of the period followed by the first mSSW. It takes place on 2 February 2016 with an increase of zonal wind speed afterwards and a second slightly stronger mSSW on 9 February 2016, again followed by a wind increase. Besides the zonal wind, GW characteristics are shown (kinematic wave energy and wave action). The small differences between kinematic wave energy and wave action are caused by the wind effect. Differences occur on dates where the zonal wind speed is high, pointing out the scaling of kinematic wave energy with the wind. A change in wave action is supposed to be caused by a variation in the intrinsic frequency hinting at a steepening of GWs.~~

~~Application of UWaDi reveals the following mean GW properties for the time period from 21 January to 21 February 2016: The horizontal wavelength ranges between 361 km and 499 km with a mean value of 414 km and shows no height dependence. This is well above the smallest sampled horizontal wavelength of about 222 km regarding the sample theorem. The vertical wavelength appears to depend strongly on the wind. Respectively, the vertical wavelength has the lower limit of 3.31 km,~~

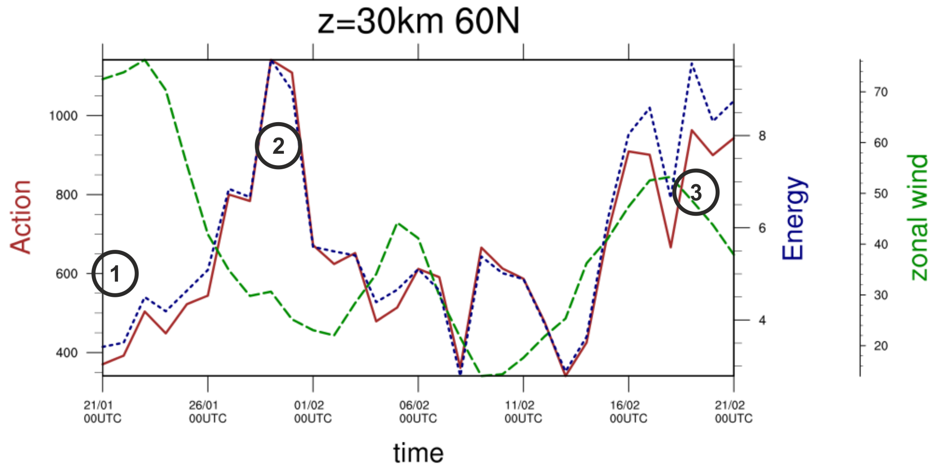

Figure 4. ~~Time series from 21 January 2016 to 21 February 2016 of wave action $\left[\mathrm{kg\,m^{-1}s^{-1}}\right]$ (red), kinematic wave energy $\left[\mathrm{m^2s^{-2}}\right]$ (blue) and zonal wind $\left[\mathrm{ms^{-1}}\right]$ (green) at 30 km altitude and 60°N. The circled numbers mark three time steps for the analysis.~~

~~which is larger than the sampling limit of 2 km. The mean intrinsic period is found to be 9.7 h. This is a typical value for near-inertial GWs, which have a frequency close to the Coriolis frequency f. The mean intrinsic phase speed is 13 $\mathrm{m\,s^{-1}}$. For the GW energy we find a mean value of 23 $\mathrm{m^2\,s^{-2}}$ in the zonal mean, while it can be locally much larger. The highest value of 690 $\mathrm{m^2\,s^{-2}}$ is found on 30 January 2016 at (60° N, 20° E). It appears in a region with high GW activity over Northern Europe (Fig. 5b).~~

~~How can the diagnosed GW properties during this minor warming be related to long-term characteristics? The horizontal wavelength appears to be slightly larger than the multi-year winter range of 238 km to 398 km as derived from radiosonde data at Lindenberg (52° N, 14° E) for the lower stratosphere (12 km to 19 km) (Schöllhammer, 2002). The vertical wavelength, instead is definitively larger than the multi-year winter mean of Lindenberg which is 2.2 km to 2.5 km. The GW energy is far above the Lindenberg values which are between 3.9 $\mathrm{m^2\,s^{-2}}$ and 7.2 $\mathrm{m^2\,s^{-2}}$. It is also far more than the maximal value of 71.8 $\mathrm{m^2\,s^{-2}}$ obtained from 10 radiosonde campaigns ran at Kühlungsborn (54° N, 12° E) (Zülicke and Peters, 2008). Do we deal with a special atmospheric situation which deviates largely from the long-term characteristics? Can we explain the diagnosed GW properties in terms of generation and propagation?~~

~~Naively, one would expect high GW activity for strong zonal mean zonal wind and vice versa. Under this aspect, three periods show interesting features (marked in Fig 4 as 1,2,3). For these three periods the stratospheric situation is reviewed (Fig. 5). Figure 5a shows the horizontal divergence and the wind velocity together with the geopotential for the prewarming case 1 on 22 January 2016 at 30 km altitude. The geopotential shows a strong polar vortex centred over the north pole with a nearly uniform distributed wind except wind deceleration areas above the USA. The horizontal divergence as an indicator~~

~~for GW activity shows features alongside the edge of the polar vortex. These patterns are described as characteristic for the prewarming phase 1 and are found in simulations, too (Limpasuvan et al., 2011). They are supposed to be westward propagating GWs excited by topography about ten days before the SSW. Observations as well as simulations declare that their wave characteristics show typical orographic features. In the upper stratosphere their vertical wavelengths are comparatively long because the short waves are filtered out by strong winds around the polar edge. In the zonal mean around the 60°-longitude and in 30 km altitude GW activity is low, while strong winds are present (Fig. 4). The polar-edge GW maximum has to be analysed locally to find comparable results to measurements in that area (Yamashita et al., 2010).~~

~~Figure 5b belongs to the period around the midwarming 2, 30 January 2016. The geopotential shows a displacement of the polar vortex coming along with a non-uniform distribution of the wind around the vortex. Wind speed is enhanced above the pole and decelerated over eastern Europe. In this area increased GW activity can be observed in the horizontal divergence field over Northern Europe. Indeed, the deceleration area of a jet stream is a possible source for GWs (O'Sullivan and Dunkerton, 1995; Zülicke and Peters, 2006; Plougonven and Zhang, 2014). This fits to the peak in wave characteristics seen in the time series (Fig. 4), although the zonal-mean zonal wind is relatively weak.~~

~~Figure 5c shows a snapshot from the postwarming phase 3, 19 February 2016. This date is characterised by a polar vortex with uniform distributed wind nearly centred above the pole. The horizontal divergence field shows much more fluctuations than on 22 January 2016 and therefore the time series (Fig. 4) shows higher values in wave characteristics in the postwarming phase. With regard to the zonal mean zonal wind, such an enhanced GW activity is expected.~~

~~Case 1 (22 January 2016)~~

~~UWaDi provides wave properties locally, hence the difference between the three selected cases can be analysed for differences in GW generation and propagation for local and zonal mean quantities. The main focus is on vertical wave propagation since the horizontal wave number can be assumed to be constant with height, which is proven in Fig. 6. It shows horizontal wave numbers corresponding to wavelengths between 359 km and 433 km. The vertical wave number is changing between zero and a corresponding wavelength of 3.2 km. Hence, the horizontal wave number variation is small and the single-column model is sufficient to explain vertical GW propagation in different wind regimes.~~

~~A longitude-height section of the zonal wind at 60° N shows the wind distribution for the 22 January 2016 in the prewarming phase 1 (Fig. 7a). The zonal wind has a strong westerly orientation in the stratosphere with a maximum above 10 hPa. The troposphere rather shows an alternating pattern caused by PWs meandering around the 60° N latitude leading to wind reversals in the troposphere. The longitude-height section of the wave action (Fig. 7b) shows enhanced GW action in the troposphere in westerlies as well as easterlies but GWs are clearly suppressed above an altitude of 19 km. In the zonal mean height-section (Fig. 7c) the zonal mean wind reversal is not strong and the wind is decreased to zero wind speed only at the surface. Wave action is strong in the troposphere, begins decreasing at 11 km altitude, right after the tropopause where a little wind minimum is visible. An even stronger decrease occurs above 19 km height which leads to a very weak GW signal in the middle stratosphere at 30 km altitude (c.f. Fig. 4). This decrease of the zonal mean action cannot be reasonably related to the increase in zonal mean wind. The zonal mean energy (Fig. 7c) peaks with the wind maximum at 36 km altitude. This finding~~

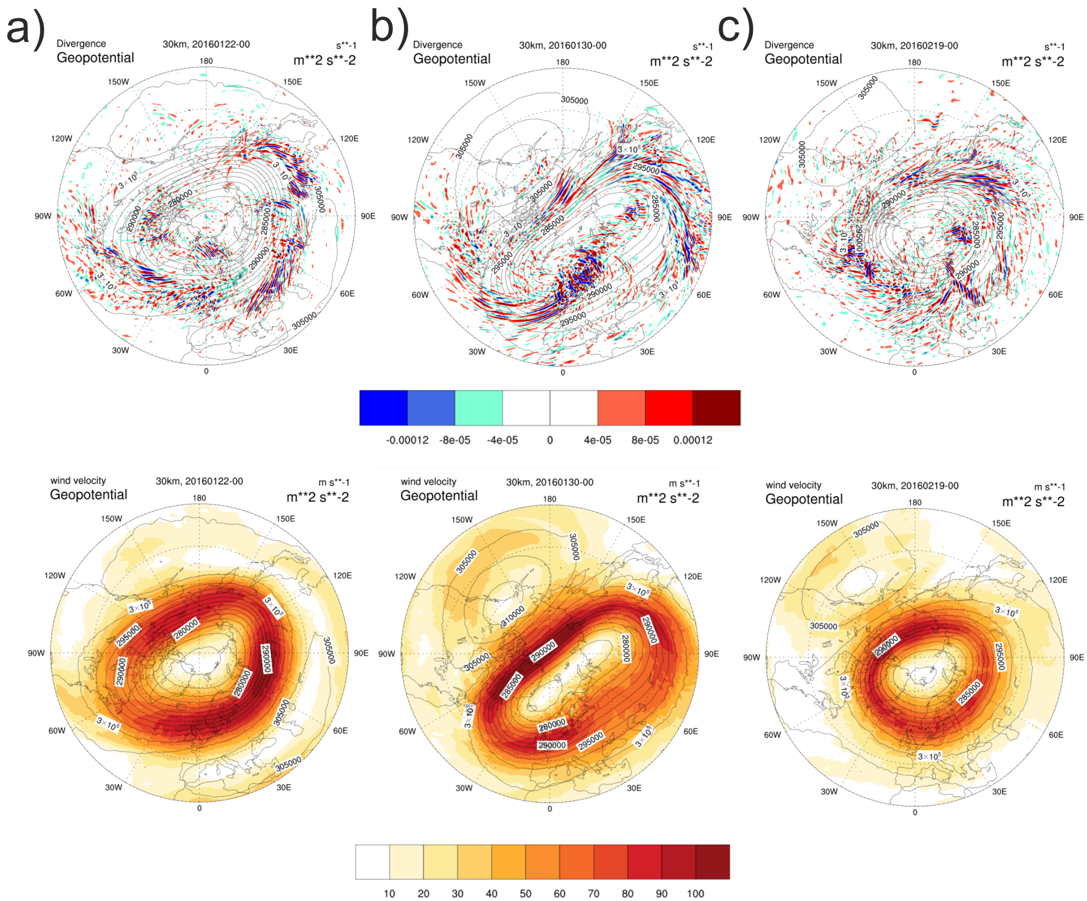

Figure 5. ~~Horizontal divergence $[\mathrm{s}^{-1}]$ (upper row) and wind velocity $[\mathrm{ms}^{-1}]$ (lower row) coloured with contours of geopotential $[\mathrm{m}^2\mathrm{s}^{-2}]$ for three time steps (columns) and 10 hPa altitude. a) 22 January 2016 1, b) 30 January 2016 2 and c) 19 February 2016 3.~~

~~contributes to our understanding to the density decrease with height which is not considered for the kinematic wave energy. Additionally, the wind effect is causing the kinematic wave energy scaling with the background wind. The downshift from the peak of kinematic wave energy to the peak of wave action can be explained by the relation between both quantities. Assuming gaussian shape distributions and looking for the maximum explains the downshift of peak from about 35 km in kinematic wave energy to about 20 km in wave action.~~

~~The local analysis provides an insight into the wind constellation with a wind reversal. A section through 50° W is shown in Fig. 7d. Instead of the kinematic wave energy the vertical wave number is plotted. In the troposphere high easterlies occur. The wind reversal takes place at 15 km height and afterwards very strong westerlies build up. These winds first filter out the westward propagating GWs in the troposphere and by changing to strong eastward winds, the eastwards propagating GWs are suppressed. Hence, ending up with very weak GW activity in the stratosphere. A first decrease in wave action is visible where $u = -15\,\mathrm{m\,s^{-1}}$ is passed, the second decrease occurs where $u \approx 15\,\mathrm{m\,s^{-1}}$ is reached at 19 km. The vertical wave number peak~~

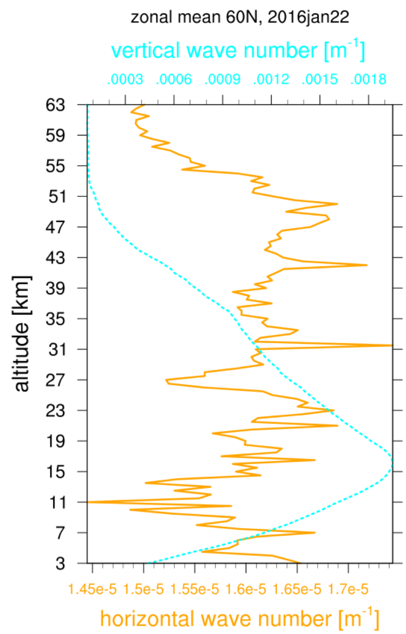

Figure 6. ~~Comparison between horizontal (orange) and vertical wave number (cyan) $[\mathrm{m}^{-1}]$ in zonal mean at 60°N against altitude for 1, 22 January 2016~~

~~is an indicator for wave absorption according to the dispersion relation and definition of the Doppler frequency: $k_z = \frac{N}{(c-u)}$. Knowing the mean horizontal phase speed of $c = \pm 13\,\mathrm{m\,s^{-1}}$, which can be calculated with the local wave properties of UWaDi, winds of this order yield to a wave number increase by reducing the denominator to zero.~~

~~Summing up, local critical-level absorption takes place in a situation with strong zonal mean zonal wind accompanied with strong PWs. In this case one can envision the valve is closed locally which leads to a decreasing zonal mean GW activity. Comparing this result to the synoptical situation shows little fluctuations in horizontal divergence at 60° N and 50° W. The polar edge with enhanced GW activity is found slightly more to the North.~~

~~Case 2 (30 January 2016)~~

~~An interesting situation with GW propagation up to the middle stratosphere is the midwarming phase 2. The 30 January 2016 shows a high peak in GW quantities although zonal wind speed is very low (Fig. 4). The longitude-height section of the zonal wind shows the mSSW features (Fig. 8a). The polar vortex displacement is visible by the easterlies in the upper stratosphere (compare Fig. 5b). The wave action in the longitude-height section shows a distinct area of propagating GWs during the SSW and areas where GWs are forbidden (Fig. 8b). The propagating area corresponds to the comparable low westerlies and forbidden zones are found where winds are very low and the wind reversal follows in higher altitudes. In zonal mean the zonal wind shows no reversal (Fig. 8c). By assessing the single-column model of vertical wave propagation, the~~

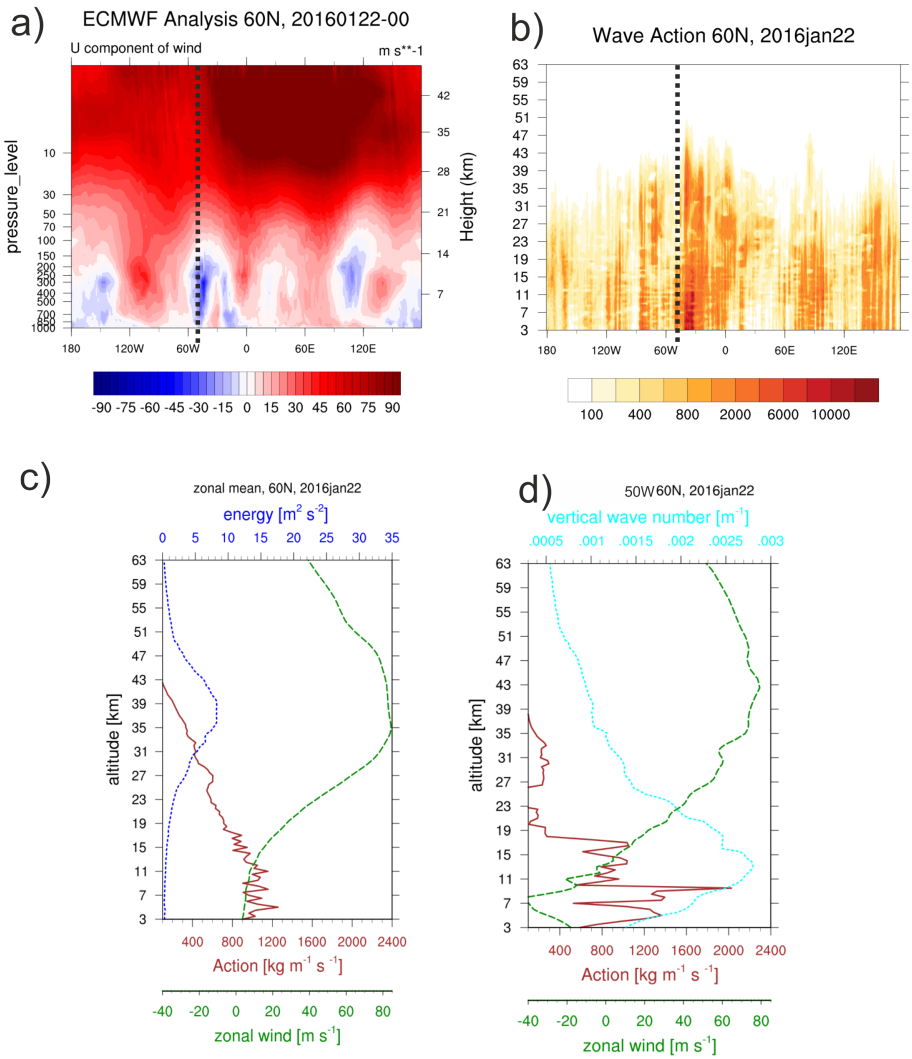

Figure 7. ~~Wave analysis for $\oplus$, 22 January 2016 at 60°N. a) Zonal wind $[\mathrm{ms}^{-1}]$ in a longitude-height cross-section. b) Wave action $[\mathrm{kg\,m}^{-1}\mathrm{s}^{-1}]$ in logarithmic scaling in a longitude-height cross-section. c) Zonal mean of wave action $[\mathrm{kg\,m}^{-1}\mathrm{s}^{-1}]$ (red), wave kinematic energy $[\mathrm{m}^2\mathrm{s}^{-2}]$ (blue) and zonal wind (green) against altitude. d) Local wave properties at 50°W. Vertical wave number $[\mathrm{m}^{-1}]$ (cyan), wave action (red) and zonal wind (green).~~

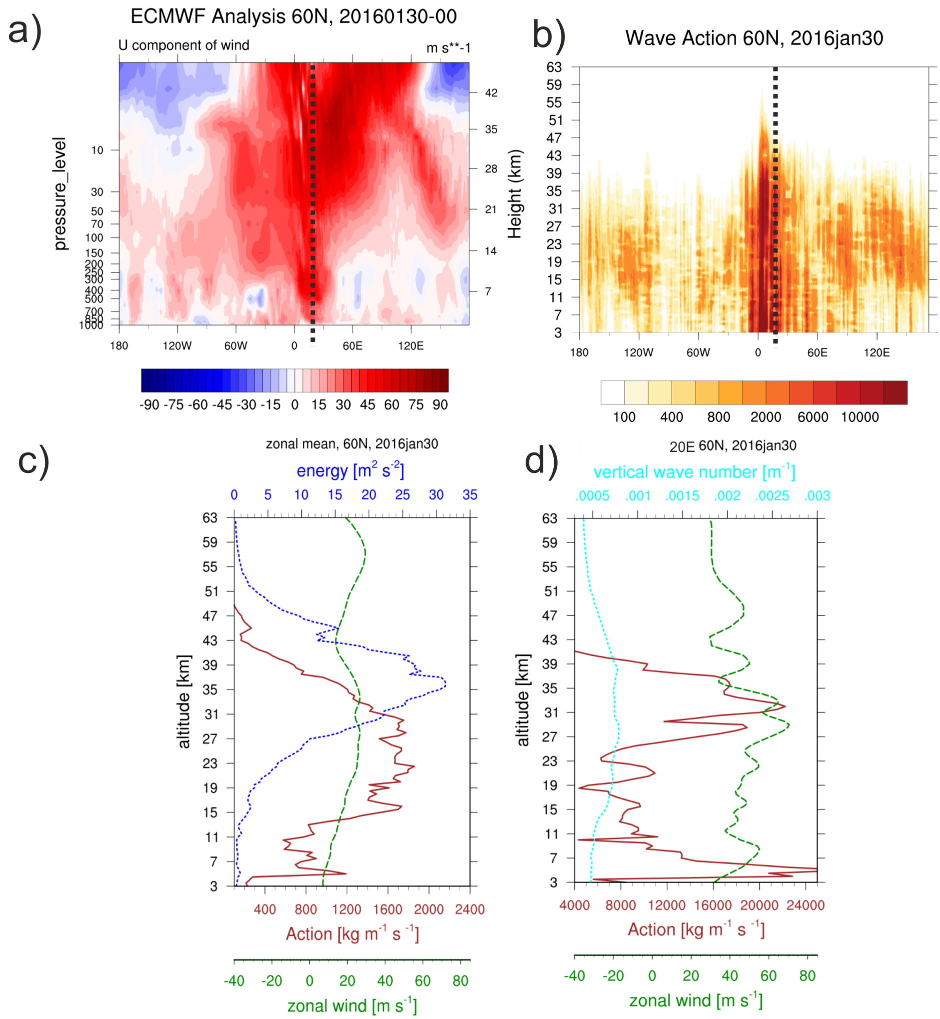

Figure 8. ~~Wave analysis for 2, 30 January 2016 at 60°N. a) Zonal wind $[\mathrm{ms}^{-1}]$ in a longitude-height cross-section. b) Wave action $[\mathrm{kg\,m}^{-1}\mathrm{s}^{-1}]$ in logarithmic scaling in a longitude-height cross-section. c) Zonal mean of wave action $[\mathrm{kg\,m}^{-1}\mathrm{s}^{-1}]$ (red), wave kinematic energy $[\mathrm{m}^2\mathrm{s}^{-2}]$ (blue) and zonal wind (green) against altitude. d) Local wave properties at 50°W. Vertical wave number $[\mathrm{m}^{-1}]$ (cyan), wave action (red) and zonal wind (green).~~

~~signals can be explained and an open valve for GW transmission is found. The midwarming phase shows higher wave action in the troposphere than during strong wind conditions (1), decreasing until the height of u_c and increasing again with further increase of wind speed. Overall, the wind speed is low and lower wave action is expected. A second wind minimum is found at 43 km but GW signals are not reliable any more in that altitude because ECMWF damping is already active.~~

~~The local analysis gives a better insight and explains the high wave action in the zonal mean. A longitudinal profile at 20° E is a case of an open valve with eastward wind over the whole height range (Fig. 8d). Clearly visible is a wave-like structure of an estimated vertical wave length of 4 km to 5 km overlaying the overall shape of the zonal wind compared to the zonal mean (Fig. 8b). This does indeed hint at strong GW activity. Instead of wind filtering and GW attenuation at the critical level, locally advantageous wind conditions allow for an effective upward propagation. Indeed, the wave guide with winds exceeding 15 ms^{-1} is 15° wide and shows a wave action peak of about 22000 $\mathrm{kg\,m^{-1}s^{-1}}$, one magnitude higher than in zonal mean. The contribution of this wave guide to the zonal mean is 1800 $\mathrm{kg\,m^{-1}s^{-1}}$ which is round-about the zonal-mean value. Hence, this local valve explains the stratospheric GW activity seen in Fig. 4.~~

~~Wave activity has its maximum at about 30 km but it is also strong in the troposphere. Such GW valve layers were already found at the southern hemisphere during the "Deep Propagating Gravity Wave Experiment" (DEEPWAVE) field campaign (Fritts et al., 2016). They act as transmission channels for GWs with small-amplitudes (Kruse et al., 2016). Other studies show the existence of the peak in GW enhancement right before the SSW but are restricted to zonal-mean measures (Yamashita et al., 2010; Jia et al., 2015). Obviously, the UWaDi algorithm can help to identify local valves explaining the GW enhancement before SSWs, when PWs are active.~~

~~Furthermore, it is shown that maximum GW amplitudes do not always correspond to areas of strongest winds by comparing the prewarming 1 and midwarming phase 2 with each other. Even though phase 2 is defined by lower wind velocities than phase 1, GWs can propagate higher during phase 2 due to an open valve. However, observations show that strongest wind areas do not always come together with high GW activity (Jia et al., 2015; Ern et al., 2016). Also for the midwarming phase 2 the ECMWF sponge layer beginning at 30 km clearly attenuates the wave activity (Fig. 8d).~~

~~Case 3 (19 February 2016)~~

~~Previous studies by measurements as well as simulations show that GW strength does not develop to comparable high values in the postwarming phase than in the prewarming phase (Yamashita et al., 2010; Ern et al., 2016). Our findings do not support this for the case study on 19 February 2016 3 (Fig. 9). This postwarming phase is characterised by high wave activity up to the middle stratosphere (Fig. 4). The wind speeds in the stratosphere are slightly weaker than in the prewarming phase 1 ($\approx 15\mathrm{m\,s^{-1}}$, see Fig. 7a and 9). However, the troposphere is more uniformly populated by westerlies meaning that the tropospheric jet meanders less around the 60° N-latitude. The wave action at the 60° N-longitude shows GW actitity broadly distributed in the middle stratosphere compared to the cases before (Fig. 9b). Especially high propagating GWs are maintained in areas of westerlies comparable to the open valve already described in phase 2.~~

~~In the zonal mean GW analysis (Fig. 9c) the zonal wind speed shows values above u_c for the whole height. Therefore GW propagation is not suppressed by wind filtering applying the single-column theory. Wave action peaks at 20 km altitude and decreases until a second local maximum at 35 km altitude. Afterwards the damping of wave on ECMWF suppresses any further propagation.~~

~~One more striking feature might be a normal case with decreasing wind in the troposphere, a clearly distributed tropospheric jet and afterwards again decreasing wind velocities in the stratosphere. This happens in the section around the 28° W-latitude,~~

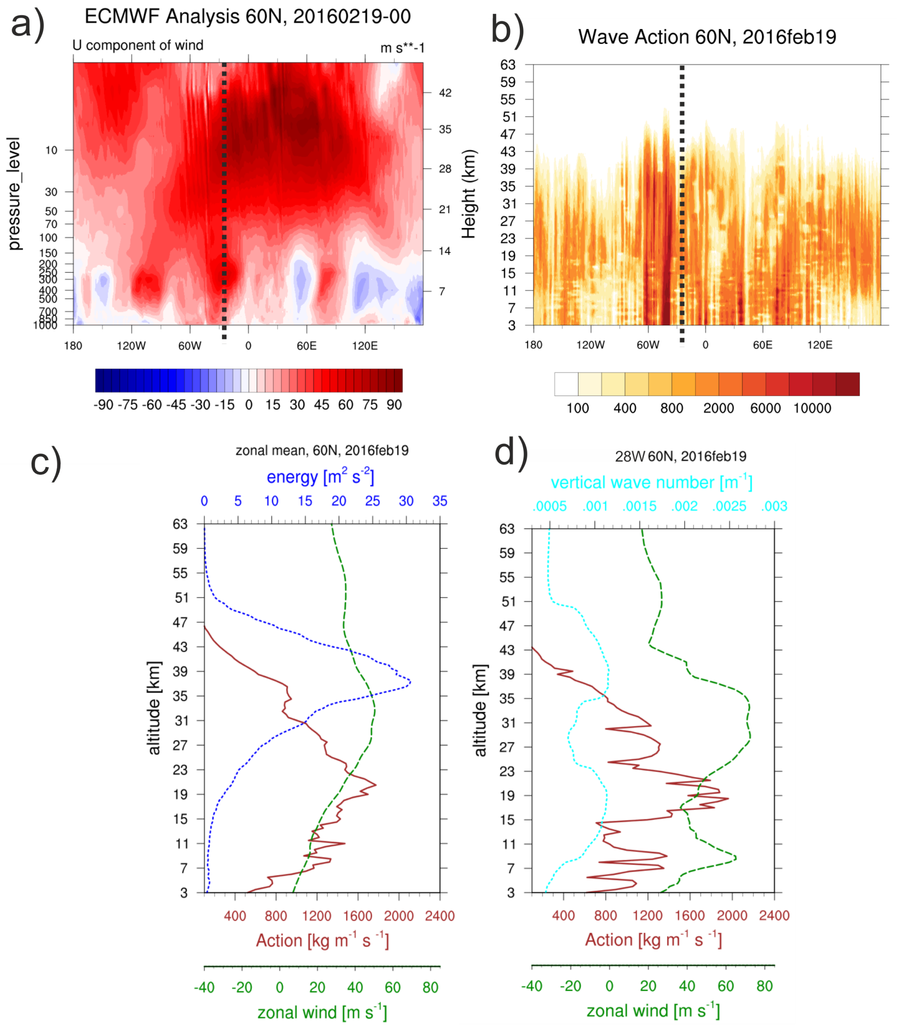

Figure 9. ~~Wave analysis for ③, 19 February 2016 at 60°N. a) Zonal wind $[\mathrm{ms}^{-1}]$ in a longitude-height cross-section. b) Wave action $[\mathrm{kg\,m}^{-1}\mathrm{s}^{-1}]$ in logarithmic scaling in a longitude-height cross-section. c) Zonal mean of wave action $[\mathrm{kg\,m}^{-1}\mathrm{s}^{-1}]$ (red), wave kinematic energy $[\mathrm{m}^2\mathrm{s}^{-2}]$ (blue) and zonal wind (green) against altitude. d) Local wave properties at 50°W. Vertical wave number $[\mathrm{m}^{-1}]$ (cyan), wave action (red) and zonal wind (green).~~

~~where a local profile is taken (Fig. 9d). The local analysis covers a height range of consistently eastward wind and additionally shows the vertical wave number. This section is characterised by a proper tropospheric and stratospheric jet. Nevertheless, the wind does not reach u_c thus GW propagation is not restrained. Wave action peaks less in the troposphere than in the stratosphere. Furthermore, a minimum can be seen in the height of the valve at about 18 km, additionally with the peak in the vertical wave number this accounts for an absorption of GWs. Wave action increases again showing that GWs still propagate vertically. It is damped by ECMWF from 30 km on. The vertical wave number peaks again at 39 km coming together with the~~

~~small peak in wave action showing another wave absorption event in that altitude but ECMWF damping obsoletes any deeper look on it.~~

~~Interestingly, the GW action in the midwarming case 2 and the postwarming case 3 is about ten times higher although the wind profiles are of similar range (compare Fig. 8d with 9d). We may speculate on different wave generation processes in these cases. Whether the source mechanism during the postwarming phase 3 is not further studied here, we have already claimed GW source for the midwarming case 2: The intense GW field near the jet-exit region over Northern Europe is a constellation preferable to spontaneous radiation of GWs.~~

A minor SSW occured on 30 January 2016. Fig. 10a shows the wind velocity of the northern hemisphere at 10 hPa. A vortex displacement from the pole is visible. The jet streak above northern Europe is decelerating. The displaced vortex causes areas of strongly curved winds. The horizontal divergence as a measure of GWs shows high wave activity above northern Europe aligned cross-stream. Equal patterns appear above eastern Siberia, corresponding to another area of a decelerating and bent wind streak. UWaDi applied on the field of horizontal divergence provides GW amplitude and wave action (Fig. 10c, d). Areas of high orography like the Tibetan Plateau and Greenland are excluded. GW amplitudes show patterns aligned with the horizontal divergence. The wave action shows the highest peak above northern Europe and lower values above eastern Siberia.

In the zonal mean the horizontal wave number remains nearly constant with increasing altitude (Fig. 11). In more convenient terms of wavelengths, we find a horizontal variation between 130 km to 165 km. The vertical wave number decreases from the bottom limit to an altitude of 3 km. At the altitude of 10 km where the tropospheric jet is expected it shows a change in gradient. The increase in vertical wave number after 35 km altitude is a feature that occurs in the zonal mean data frequently, independent from the overall synoptic situation and is therefore expected to be an artefact of artifical wave damping from the IFS sponge layer. In wavelength, the vertical wave number in zonal mean varies between 2 km and 5 km.

We next inspect local profiles in different background wind conditions. Longitude-height sections of zonal wind (Fig. 12a) and wave action (Fig. 12b) at 60° N on 30 January 2016 help to find the location of interesting vertical profiles. Three profiles are chosen that are representative for regions of similar filter conditions. We did not find significant differences between spatial averaging over areas of some longitudes extension and the local profiles (not shown). The low-pass filter applied in Step 8 helps to overcome massive grid-point to grid-point fluctuations. The first profile 1 at 7.56° E is chosen to be in a height range characterised by strong zonal eastward winds and lies in the deceleration area of the jet stream above northern Europe. Profile 2 is at 151.92° E, therewith in the area of a descented stratospheric jet streak caused by the displacement of the polar vortex. In Fig. 12a it is visible as a wind intrusion in the altitude range between 14 km and 34 km. The wave action shows a peak in that height area (Fig. 12b). For comparison we take a third profile 3 at 240.12° E in a region of low wind velocity, that is: weak tropospheric and weak stratospheric jets.

To highlight the advantage of a local wave analysis we plot the zonal mean wave quantities at 60° N on 30 January 2016 (Fig. 13a). One can see the energy scaling with the decreasing density with increasing altitude. Small deviations from the

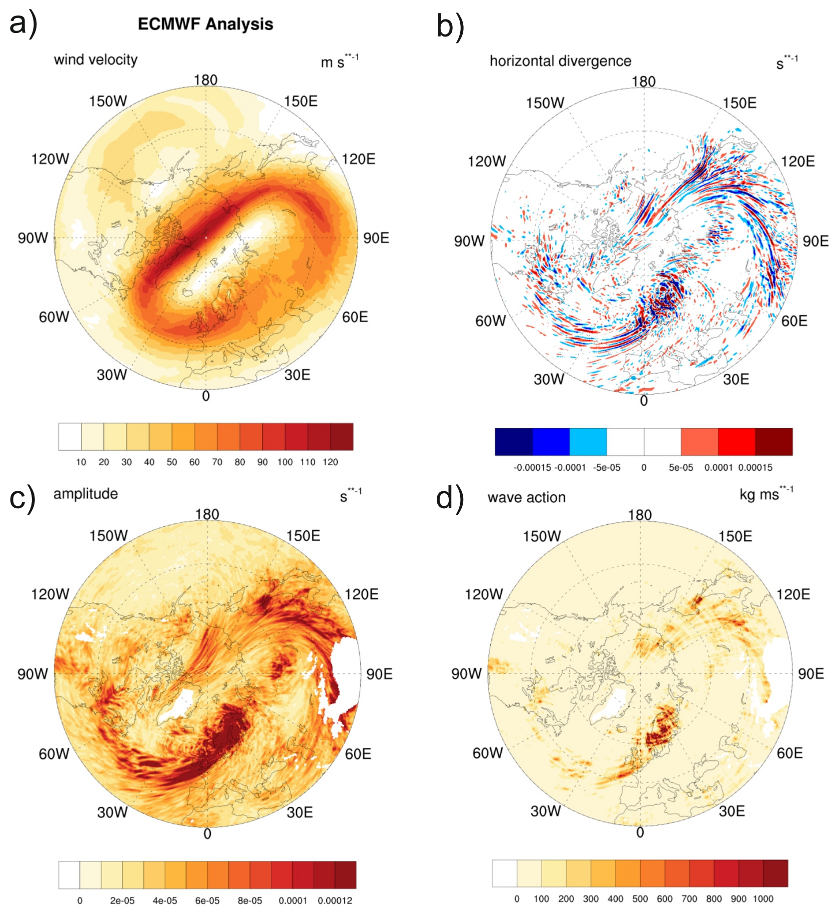

Figure 10. Synoptical situation of the northern hemisphere from ECMWF analysis at 10 hPa on 30 January, 2016. Wind velocity (a), horizontal divergence (b). Gravity wave amplitude (c) and wave action (d).

exponential density structure correlate with small jumps in the wave action profile. Overall, zonal mean zonal wind is low with a small maximum hinting at the stratospheric jet stream. Wave action and kinematic wave energy are highly variable below 6 km altitude because of orographic influence. The not trustworthy areas are excluded. Overall, wave action decreases from 1000 $\mathrm{kg\,m^{-1}\,s^{-1}}$ in the upper troposphere to 100 $\mathrm{kg\,m^{-1}\,s^{-1}}$ in the middle atmosphere. Further upwards it remains constant. A constant profile of wave action means a constant propagation of GWs without deposition of momentum and therefore no interaction with the mean flow. The wind profile shows low wind speeds. We are interested in selective wave transmission which can not be seen from zonal mean averages. Thus, we provide local profiles.

During a local increase of wind velocity above northern Europe the vertical profiles of 1 show that the zonal wind meanders around 50 $\mathrm{m\,s^{-1}}$ (Fig. 13b). The vertical wave number is nearly constant with an average wave length of 8 km and a small minimum after the tropospheric jet with 7 km. The low-pass filter acts on a spatial running average of $k_{min} = 15\mathrm{km}$, therefore

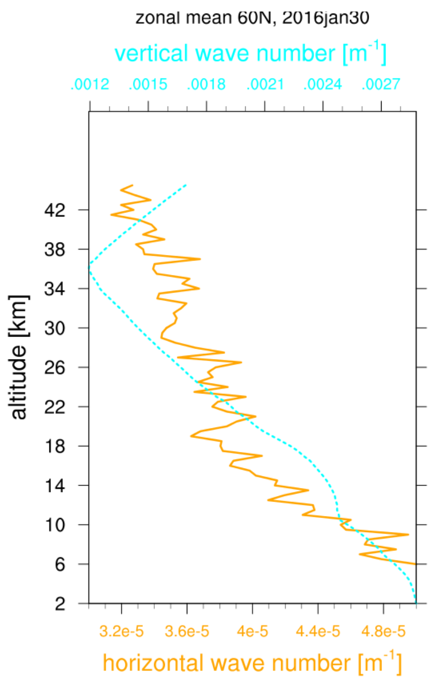

Figure 11. Horizontal (solid, orange) and vertical (dotted, light blue) wave number in zonal mean at 60°N, on 30 January 2016.

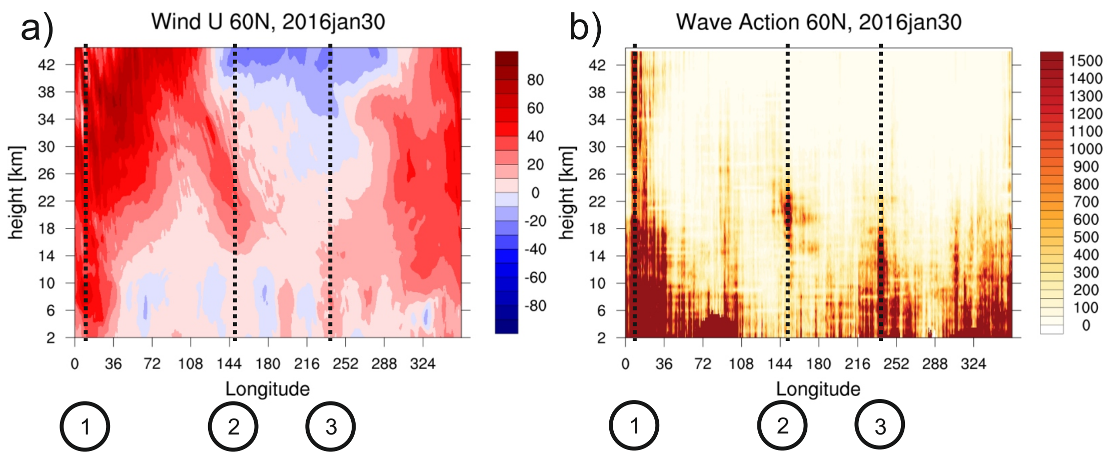

Figure 12. Zonal wind (a) and wave action (b) at 60°N, 30 January 2016 in longitude-height section. Numbered vertical profiles for further analysis are highlighted.

the wave number does not scale with the wind fluctuations. The wave action shows a high gradient changing from former $10000\,\mathrm{kg\,m^{-1}\,s^{-1}}$ to $1000\,\mathrm{kg\,m^{-1}\,s^{-1}}$, right where the vertical wave number has its maximum at an altitude of $16\,\mathrm{km}$.

Above eastern Siberia a descended stratospheric jet streak appears, jointly with high wave action (Fig. 12). The zonal wind vertical profile 2 shows this in a height range of $14\,\mathrm{km}$ to $30\,\mathrm{km}$ with in increase from $5\,\mathrm{m\,s^{-1}}$ to maximal $30\,\mathrm{m\,s^{-1}}$ (Fig. 13c). The wave action follows the structure of the zonal wind. The vertical wave number shows lower gradients in that altitude range. Altogether, GW emissions seems to take place in the lower stratosphere, clearly above the tropospheric jet stream. GWs of vertical wave length of $2\,\mathrm{km}$ can be found.

The last set of vertical profiles is located in an area of low zonal winds 3 (Fig. 13d). In the troposphere eastward winds and in the middle stratosphere westward winds occure. In the altitude of the wind reversal a change of gradient in wave action might show a filter process of GWs. This profile lies in the lee of the Rocky Mountains, hence, mountain waves are most likely.

4 Discussion

The topic of selective wave transmission was first risen up by Dunkerton and Butchart (1984). They highlighted the longitude-dependent gravity wave propagation during a SSW by focussing on the impact on the mesosphere. Ern et al. (2016) further point out that the selective filtering by the anomolous winds during a SSW create heavy impact on GW propagation through the whole atmosphere. They point out theoretically, that during the upwards propagation of GWs, these waves get attenuated or eliminated by distinct specifications of background flows. These findings were obtained with the box-based S-3D algorithm. We add some spatially more refined analysis with UWaDi.

The high-wind case 1 showing the highest values of wave action and nearly no changes in the vertical wave number above northern Europe are defined by the longest vertical wave length with $7\,\mathrm{km}$. This long vertical wave length describing steep waves may hint on an orographic excited GW caused by the eastward flow above the scandinavian mountain ridge Kjølen. The location as well as the filtered out short vertical wave lengths suggest this idea and agree with findings of Limpasuvan et al. (2011). The overall high wave action underlines the orographic induced GW packet assumption. This is close to the findings of Krisch et al. (2017), who analysed a wave packet on 25 January 2016 above Iceland, just a few days before our analysis. Mentionable is that from the 25 January to 30 January the overall approaching flow direction did not change above northern Europe and comparable GW characteristics can be expected. Further detailed analysis on this GW packet are expected by upcoming publications according to the joint measurement campaign of METROSI, GW-LCYCLE 2 and PACOG at, amongst others, Kiruna, Sweden (67° N, 20° E).

In the descended stratospheric jet case 2 (Fig. 13c) we find a GW packet triggered off a bent and decelerating stratospheric jet. Firstly explained by Uccelini and Koch (1987), jet-exit regions in the troposphere are expected to emit GWs. The increase of wave action in the middle stratosphere according to the intrusion of westerlies seen in Fig. 12a and b leads to the assumption that the present feature is caused by the stratospheric jet. The horizontal divergence field supports this hypothethis with cross-stream aligned fluctuations above eastern Sibera, comparable to the findings in the troposphere by Mirzaei et al. (2014). Further agreements are the higher wave action as well as the lowest shown wavelength in this case of $1.9\,\mathrm{km}$. Wave packets found in

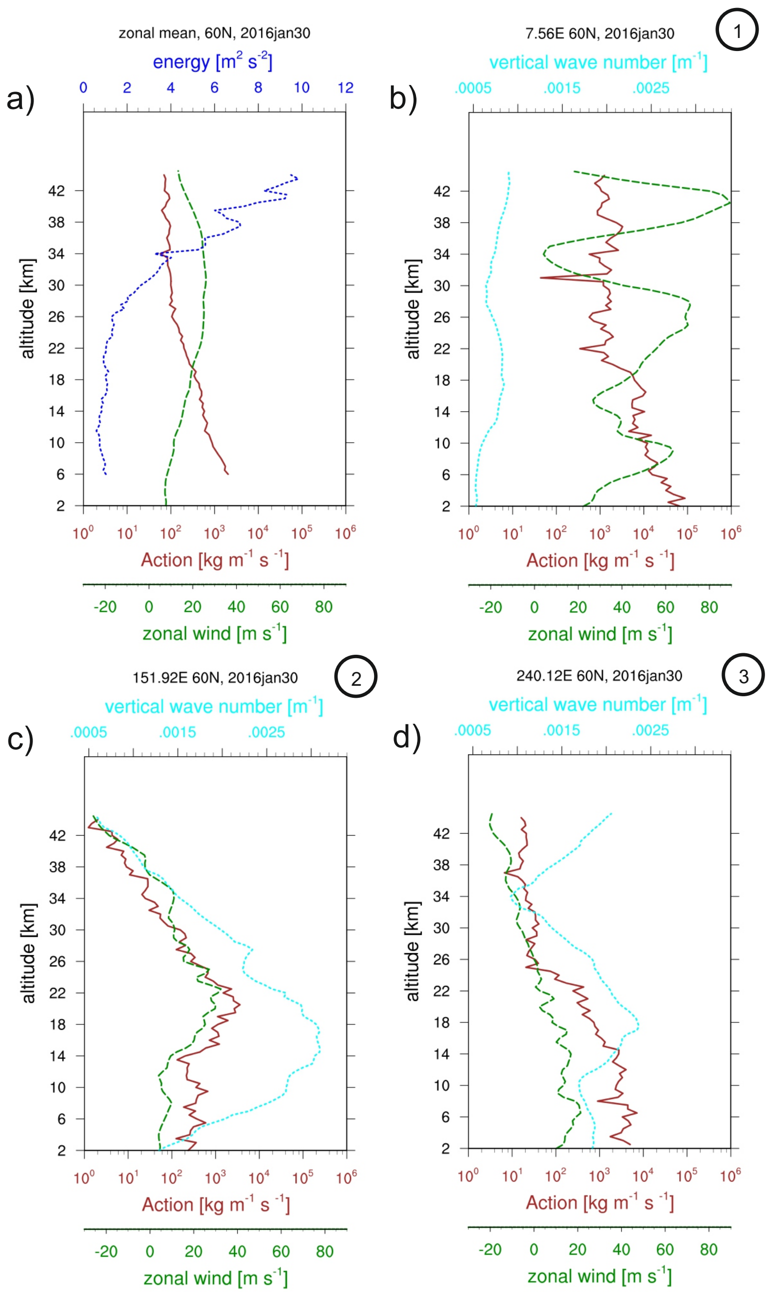

Figure 13. Vertical profiles at 60°N, 30 January 2016. Zonal mean (a) of kinematic wave energy (dotted, blue), wave action (solid, red) and zonal wind (dashed, green). Local vertical profiles at 7.56°E (b), 151.92°E (c) and 240.12°E (d) with the vertical wave number (dotted, light blue), wave action (solid, red) and zonal wind (dashed, green). Local profiles according to markers of Fig. 12.

jet-exit region are characterised as shallow near-inertial wave packets.

Furthermore, we want to discuss the phenomenon of vanishing GWs at critical wind levels. Stating that waves orthogonal to the mean flow are eliminated due to critical layer absorption occures if the wave vector rotates (Dunkerton and Butchart, 1984). With local vertical profiles of the vertical wave number we find these features above the descended stratospheric jet in 2. The critical level is the level at which background wind and GW phase speed are of same value. There, GWs dissipate and drag is put on the mean flow at lower altitudes than during undisturbed conditions (Wang and Alexander, 2009). Here, a peak in vertical wave number is an indicator for wave absorption according to the mid-frequencies dispersion relation and definition of the Doppler frequency: $k_z = \frac{N}{(c-u)}$. At winds of the order of the phase speed the denominator reduces to zero and the vertical wave number peaks. In an altitude of 28 km we see a peak in the vertical wave number where the zonal wind reaches $u \approx 15 \mathrm{m\,s^{-1}}$. We find a horizontal phase speed of $c \approx 15 \mathrm{m\,s^{-1}}$, which measures up with the expectations because jet-generated GWs tend to be fast. The decrease of wave action quantifies the filtering of GWs in this height range. A sharp jump to less wave action is not expected as we apply the low-pass filter and it may take the length of one wave to be filtered out. Furthermore, due to the relative high phase speed no sharp variation at the height of the wind reversal is visible. The near-inertial GWs are not subject of absorption.

In the low-wind case 3 we see that the vertical wave number does not directly scale with the low zonal wind. The high wave action in the upper troposphere up to the height of the wind reversal of 23 km may be caused by orographic induced GWs due to the position in the lee of the Rocky Mountains. Assuming to have orographic quasi-stationary GWs, we get a horizontal phase speed of $c \approx 0 \mathrm{m\,s^{-1}}$ and do not find absorption at critical levels except at the height of the wind reversal, where a high gradient in wave action is visible. Above that, the overall lowest values of wave action are found, aggreeing with measurements in that height range (Thurairajah et al., 2010). The feature of increasing vertical wave number above an altitude of 35 km fits to our findings before, where in zonal mean vertical wave number we saw the sponge layer of the model to begin to act on GWs (Fig. 11). We suggest, the fact that we do not see this in the other profiles arises from the low wind speeds jointly with low phase speed for this case. In zonal mean we do find low zonal winds as well (Fig. 13a).

5 Summary and Conclusion

~~A diagnostic tool for studies of wave packets is developed and applied. The Unified Wave Diagnostics (UWaDi) uses the Hilbert Transform to obtain a complex signal from a real-valued function and estimates the amplitude and wave number locally. Although applicable to any wave-like signal, we specified it to detect gravity waves. The procedure leads to reliable results for synthetic test cases and operational analysis data. The lack of sign of the estimated wave numbers by UWaDi can be overcome by implementing a frequency-wave number analysis. This will help improving the understanding of GW propagation, whereas directions of propagations can be put into relation to the background wind vector.~~

~~The analysis of ECMWF-IFS data shows resolved GWs in the troposphere and stratosphere. However, above an altitude of 1 hPa no systematic waves could be found and even above 10 hPa the first sponge layer starts and the results have to be interpreted with care. We use these data to demonstrate the different patterns of wave action and wave energy. As expected, the~~

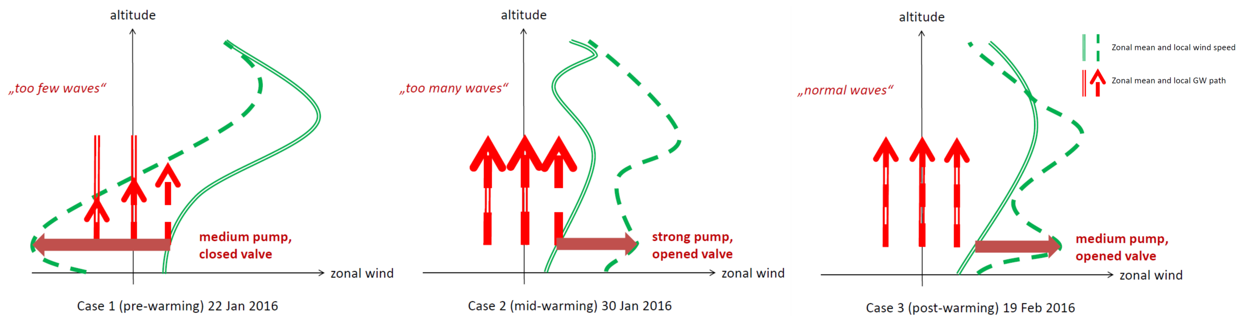

Figure 14. ~~Schemes of GW paths (red) and zonal wind (green) for zonal mean (bold line) and locally (dashed) for phase 1, 2 and 3.~~

~~kinematic wave energy strongly depends on density and wind profiles and might establish a maximum while the wave action does not peak at this location. We have shown this for zonal-mean profiles and decided to use the wave action for the wave analysis.~~

~~We study a minor sudden stratospheric warming (mSSW) event including strong zonal wind variations in space and time. The usual expectation is that high zonal-mean zonal wind causes high wave activity. We analysed three different situations and identified valves and pumps of GWs. First, a low-wind region near the tropopause causes low GW action while the stratospheric wind is high during the prewarming phase 1. This is an example for a closed valve (Fig. 14-1). Second, better propagation conditions are found during the midwarming phase 2, where an open local valve with high westerlies in a situation when the stratospheric wind is low, makes it possible for GWs to propagate into the stratosphere and cause GW action substantially higher than in any other period. Additionally, the GW generation in the troposphere was found to be enhanced. Hence, the GW pump was running high (Fig. 14-2). Third, GW propagation was also analysed for the postwarming phase 3 where the mid-stratospheric wind reinforced again and GW action is smaller than during the midwarming phase 2. Here, both the zonal mean and the local wind fields permitted GW propagation and the stratospheric wave activity was passing the valve as expected while the GW pump was running normal (Fig. 14-3). These three cases demonstrate that for the evaluation of GW activity at a certain altitude its whole propagation history through the layers below has to be taken into account. In particular during SSWs the structure of PWs may modify the local GW generation (pump) and transmission (valve) considerably.~~

~~In some cases (2,3) we detected secondary peaks in the wave action profiles. This might be associated to non-tropospheric wave generation. Possible candidates are the tropospheric and the stratospheric jet. These two cases are also described by similar wind conditions but different wave distributions which also might be due to different wave generation processes. It was just the midwarming case 2 at 30 January 2016 at 60° N 20° W for which we found an extraordinarily high GW activity at 10 hPa. This occasion was also covered by the ROMIC/GW-LCYCLE campaigns and might deserve special attention.~~

~~Besides the particular application of UWaDi to GWs and SSWs, the tool was already successfully tested to identify wave packet properties in rotating annulus experiments Hien et al., 2017. Recapitulatory, the study of SSW is a good test case for GWs due to the high spatio-temporal variability due to PW activity. This changes not only the propagation conditions locally in a drastic way, but also gives rise to changing wave generation.~~

With UWaDi we provide a tool for the analysis of any wave-containting data to estimate amplitude and wave number phase-independent and locally. The method is based on a Hilbert transform and returns such an estimate for each data grid point, thus, avoiding the use of pre-defined boxes for a spectral estimate. With regard to the locality it clearly shows its advantages in a method comparison for an synthetic test case. Disadvantages may play a role when the wave spectrum is broad and the nomination of one dominant harmonic is not justified. The additional estimation of the wave numbers completes the elements of a wave packet description. Their sign is not fixed which is the case for all spatial analysis methods. However, the method is recommended as a reliable local estimate of medium complexity.

For the analysis of gravity waves, we estimated wave energy and wave action from the horizontal divergence. This approach does not require an explicit numerical filtering which is a practical advantage. Other methods for the analysis of unbalanced flow components are available, although more complicated (Mirzaei et al., 2017). While the chosen formulae requires the variance (or squared amplitude) and wave numbers, UWaDi may also provide local estimates for more complex tools such as the combined Rossby wave and gravity wave diagnostics of Kinoshita and Sato (2013). There, cross-covariances of different quantities are needed. For our study, which is focused on GWs, the specific approach is optimal.

With the short analysis of the synoptic situation on 30 January 2016 we show the advantages of UWaDi: providing wave quantities on every grid point. Longitude-dependent GW filter processes, known as selective wave transmission, can be analysed in detail. We find that in zonal mean no prominent GW features can be seen during a mSSW vortex displacement. Instead, local vertical profiles show selective wave transmissions relative to the zonal mean profiles. During strong eastward winds GW propagation is high at all altitudes, the vertical wave number does not show strong variation, thus indicating a steadily vertical propagation of GWs. We find the source of the GWs in the troposphere and characterise this case as induced by flow over orography. Further, critical layer absorption is visible. The wave case with overall low zonal wind reveals gradients in wave action at the altitude of a wind reversal. Unexpectingly, we see the influence of the ECMWF sponge layer in the stratosphere which starts to flatten GWs at an altitude of 35 km in situations of weak winds and slow waves. In an area where the wind field is effected by the mSSW, we find a curved and decelerating jet stream-exit region in the stratosphere and suggest that GWs are emitted there. With the present method we plan to join the closer evaluation of observations and models with respect to local features of GW generation and propagation.

Code and data availability. The data from ECMWF is accessible through the archive of www.ecmwf.int provided by the Deutscher Wetterdienst. The code named UWaDi is available through the authors. It is coded in open-source software and an user's manual is provided. The authors request to cite this paper in case of applying the UWaDi algorithm.

Appendix A: Estimates for two-wave mixture

In this section we illustrate mathematically the amplitude and wave number estimate for a superposition of waves. For simplicity, imagine a mixture of two waves

$$f = a_1 \cos(k_1 x + \phi_1) + a_2 \cos(k_2 x + \phi_2). \tag{A1}$$

The Hilbert transform creates

$$H = a_1 \sin(k_1 x + \phi_1) + a_2 \sin(k_2 x + \phi_2). \tag{A2}$$

The amplitude is calculated by

$$a^2 = f^2 + H^2 \tag{A3}$$

and contains mixed-wavelengths which are either slow $(\pm(k_1 - k_2))$ or fast $(\pm(k_1 + k_2))$. The application of the low-pass filter (Step 8) is intented to eliminate the fast spurious components which are expected to create the most fuzziness. With this procedure supposed to work we find from the equal-wave number termn the sum of all squared amplitudes

$$a^2 = a_1^2 + a_2^2. \tag{A4}$$

This means: all variance is included in this estimate. For the wave numbers we find from the definition

$$k^2 = \frac{k_1^2 a_1^2 + k_2^2 a_2^2}{a_1^2 + a_2^2}. \tag{A5}$$

This is the amplitude-weighted sum of squared wave numbers.

The covariance (or squared standard deviation) is the mean of squares:

$$s^2 = \langle f^2 \rangle = \langle a_1^2 \cos^2(k_1 x + \phi_1) + a_2^2 \cos^2(k_2 x + \phi_2) \rangle = \frac{a_1^2}{2} + \frac{a_2^2}{2} = \frac{a^2}{2} \tag{A6}$$

Hence, the ensemble average results in half of the squared amplitude.

Appendix B: Derivation of kinematic wave energy

The total energy is composed of kinetic and potential energy ($e_{tot} = e_{kin} + e_{pot}$). We use the polarisation equations for hydrostatic GWs to express the kinetic energy with horizontal divergence $\delta = -\mathrm{i}(k_x u + k_y v)$ and vorticity $\xi = -\mathrm{i}(k_x u - k_y v)$ as

$$e_{kin} = \frac{1}{2}(u^2 + v^2) = \frac{1}{2}\frac{\delta^2 + \xi^2}{k_h^2}. \tag{B1}$$

The potential energy is expressed with the buoyancy tendency $-\mathrm{i}\omega b = -N^2 w$ to yield

$$e_{pot} = \frac{1}{2}\frac{b^2}{N^2} = \frac{1}{2}\frac{N^2 w^2}{\omega^2} \tag{B2}$$

in order to express the total energy in terms of the divergence, both formulae are combined with the vorticity tendency $-\mathrm{i}\xi = -f\delta$ and the continuity equation $(\delta = \mathrm{i}k_z w)$ for

$$e_{tot} = \frac{1}{2}\left(\frac{\delta^2}{k_h^2}\left(1 + \frac{f^2}{\omega^2}\right) + \frac{N^2}{\omega^2}\frac{\delta^2}{k_z^2}\right). \tag{B3}$$

The final result is obtained with incorporation of the disperion relation $\omega^2 = f^2 + N^2\frac{k_h^2}{k_z^2}$ reading

$$e_{tot} = \frac{\delta^2}{k_h^2}. \tag{B4}$$

Competing interests. The authors declare that no competing interests are present.

Acknowledgements. We acknowledge the funding of the research unit Multiscale Dynamics of Gravity Waves / project Spontaneous Imbalance by the Deutsche Forschungsgemeinschaft (DFG) through grant ZU 120/2-1. Furthermore the authors want to thank the ECMWF for data supply ~~and the WRF user support at NCAR for the assistance provided with the data processing with WPS.~~ Useful comments on this manuscript were given by Vivien Matthias and Steffen Hien.

References